

**Figure 4** Transgastrostomic endoscopy during retrograde passage showing (a) no recurrence after chemoradiation therapy for advanced esophageal cancer and (b) recurrence of esophageal cancer with stenosis.

duodenal ulcer scar. It is thought that the PEG buttons that were used in most of the patients were not long enough and that they did not compress the posterior wall of the gastric body.

In our study, malignant tumors, such as early-stage gastric cancer and recurrent esophageal cancer, could be detected and they were diagnosed with biopsy specimens. Although most patients who have undergone PEG have comorbid illness, it is useful for some patients in relatively good condition to detect early-stage gastric or esophageal tumors and to treat them endoscopically as a minimally invasive treatment.<sup>14</sup>

It was easy to observe the gastrostomy site in the stomach in retroversion in all examinations, so all sites in the stomach could be observed. Biopsy specimens could be taken in any site in the stomach, even in the gastrostomy site. The mean operating time of the endoscopic procedure was less than 5 min, and no complications occurred. Although this procedure was performed in only a single center, observation of the upper GI tract with TGE using the ultrathin endoscope during the PEG button or tube replacement is thought to be efficacious and safe.

For unconscious patients, only local anesthesia of the gastrostomy site due to the application of lidocaine hydrochloride jelly was needed to make the PEG button replacement and the endoscopic procedure through the gastrostomy tract painless. None of the conscious patients needed intravenous pethidine to reduce abdominal pain for the endoscopic procedure, but some needed it for the PEG button replacement.

The thin endoscope Nishiwaki used requires a gastrostomy tract large enough for a 24-Fr PEG button,<sup>13</sup> but the ultrathin endoscope we used needs a tract large enough for a 20-Fr PEG button. As the diameter of the XP260N is smaller than that of the gastrostomy tract suitable for a 24-Fr PEG button, it is necessary to fill the gap

between the endoscope and the gastrostomy tract with gauze in order to prevent leakage of air out of the stomach.

In conclusion, observation of the upper gastrointestinal tract with transgastrostomic endoscopy using an ultrathin endoscope during a gastrostomy button or tube replacement may be useful and safe.

### Competing interests

The authors declare that they have no competing interests.

### References

- 1 Ponsky J, Gauderer M. Percutaneous endoscopic gastrostomy: a nonoperative technique for feeding gastrostomy. *Gastrointest. Endosc.* 1981; **27**: 9–11.
- 2 Tokunaga T, Kubo T, Ryan S *et al.* Long-term outcome after placement of a percutaneous endoscopic gastrostomy tube. *Geriatr. Gerontol. Int.* 2008; **8**: 19–23.
- 3 Ono H, Azuma T, Miyaji H *et al.* Effects of percutaneous endoscopic gastrostomy tube placement on gastric antral motility and gastric emptying. *J. Gastroenterol.* 2003; **38**: 930–6.
- 4 Kitamura T, Nakase H, Iizuka H. Risk factors for aspiration pneumonia after percutaneous endoscopic gastrostomy. *Gerontology* 2007; **53**: 224–7.
- 5 Hsu YC, Tsa JJ, Perng CL, Lin HJ. Massive gastrointestinal bleeding associated with contralateral mucosal abrasion by percutaneous endoscopic gastrostomy tube. *Endoscopy* 2009; **41**: E144.
- 6 Kanie J, Akatsu H, Suzuki Y, Shimokata H, Iguchi A. Mechanism of the development gastric ulcer after percutaneous endoscopic gastrostomy. *Endoscopy* 2002; **34**: 480–2.
- 7 Trevisani L, Cifala V, Sartori S, Gilli G, Matarese G, Abbasciano V.

- Unsedated ultrathin upper endoscopy is better than conventional endoscopy in routine outpatient gastroenterology practice: a randomized trial. *World J. Gastroenterol.* 2007; **13**: 906–11.
- 8 Itoi T, Kawai T, Itokawa F *et al.* Initial experience of transnasal endoscopic biliary drainage without conscious sedation for treatment of acute cholangitis (with video). *Gastrointest. Endosc.* 2008; **67**: 328–32.
- 9 Kanno Y, Hirasawa D, Fujita N *et al.* Long-tube insertion with the ropeway method facilitated by a guidewire placed by transnasal ultrathin endoscopy for bowel obstruction: a prospective, randomized controlled trial. *Gastrointest. Endosc.* 2009; **69**: 1363–8.
- 10 Lustberg A, Fleisher AS, Darwin PE. Transnasal placement of percutaneous endoscopic gastrostomy with a pediatric endoscope in oropharyngeal obstruction. *Am. J. Gastroenterol.* 2001; **96**: 936–7.
- 11 Vitale MA, Villotti G, D'Alba L, De Cesare MA, Frontespezi S, Iacopini G. Unsedated transnasal percutaneous endoscopic gastrostomy placement in selected patients. *Endoscopy* 2005; **37**: 48–51.
- 12 Adler DG, Gostout CJ, Baron TH. Percutaneous transgastric placement of jejunal feeding tubes with an ultrathin endoscope. *Gastrointest. Endosc.* 2002; **55**: 106–10.
- 13 Nishiwaki S, Araki H, Niwa Y *et al.* Usefulness of transgastrostomic endoscopy (TGE) in patients with percutaneous endoscopic gastrostomy (PEG). *Gastroenterol. Endosc.* 2005; **47**: 49–55 (Japanese, abstract in English).
- 14 Nishiwaki S, Araki H, Shirakami Y *et al.* Transgastrostomic endoscopy-assisted endoscopic submucosal dissection. *Endoscopy* 2009; **41**: E13.
- 15 Mori A, Ohashi N, Maruyama T *et al.* Endoscopic retrograde cholangiopancreatography through a gastric stoma using an ultrathin endoscope: a novel approach. *Endoscopy* 2007; **39**: E323.

## Two Amino Acids Mutation of Ferric Uptake Regulator Determines *Helicobacter pylori* Resistance to Metronidazole

Hitoshi Tsugawa,<sup>1</sup> Hidekazu Suzuki,<sup>1</sup> Kazue Satoh,<sup>2</sup> Kenro Hirata,<sup>1</sup> Juntaro Matsuzaki,<sup>1</sup> Yoshimasa Saito,<sup>1</sup> Makoto Suematsu,<sup>3</sup> and Toshifumi Hibi<sup>1</sup>

### Abstract

Metronidazole (Mtz) is a prodrug that is converted to its active form when its nitro group is reduced and superoxide radicals are generated. The superoxide radicals are directly toxic to the bacterium. On the other hand, the transcriptional regulator, ferric uptake regulator (Fur), of *Helicobacter pylori* is a direct suppressor of the iron-cofactored superoxide dismutase SodB, which is essential for protection against superoxide attack. Here, we demonstrate that in some Mtz-resistant strains, SodB activity is induced in a dose-dependent manner on exposure to Mtz. Further, under Mtz exposure, the generation of superoxide radicals in Mtz-resistant strains was significantly reduced as compared with that in the Mtz-susceptible strains. These Mtz-resistant strains were found to carry amino acids mutation of Fur (C78Y, P114S; mutant-type Fur). The binding affinity of the mutant-type Fur to an operator sequence on the *sodB* promoter (Fur-Box) was significantly reduced. Our approach demonstrated that SodB expression is derepressed by mutant-type Fur, which is associated with the development of Mtz resistance. *Antioxid. Redox Signal.* 14, 15–23.

### Introduction

**H**ELICOBACTER PYLORI IS A GRAM-NEGATIVE BACTERIUM that colonizes the gastric mucosa in more than half of the entire population of the world; it is a major cause of chronic active gastritis and peptic ulcer disease and also an early risk factor for gastric cancer (16, 43). Eradication of this bacterium from the stomach results in recovery from gastritis and peptic ulcer disease in over 90% of patients. Metronidazole (Mtz) was initially used against a variety of anaerobic microorganisms, but the drug was later found to also exhibit activity against certain microaerophilic organisms such as *H. pylori*. Currently, one of the most effective treatment regimens for *H. pylori* consists of a combination of a proton pump inhibitor and any two of the following three antimicrobial agents: amoxicillin, Mtz, and clarithromycin (15).

Recently, a gradually increasing prevalence of Mtz resistance has begun to be reported from Asia and Europe (11, 26, 47). Kim *et al.* suggested that Mtz is also widely prescribed for other infections such as parasitic or genital infections and that such widespread use and abuse of this inexpensive drug may contribute to the increasing prevalence of Mtz resistance (26). This increase in the prevalence of Mtz resistance is likely to become an issue of concern in the clinical management of

*H. pylori* infection. Mtz enters the cells by diffusion, and its antimicrobial toxicity is dependent on the reduction of its nitro group to nitro anion radicals and the generation of superoxide radicals (37, 38). According to Goodwin *et al.*, since nicotinamide adenine dinucleotide phosphate (reduced form) nitroreductase (RdxA) of *H. pylori* reduces the nitro group of Mtz to anion radicals that produce DNA strand breaks and oxidative stress, which ultimately cause rapid cell death (14), mutational inactivation of the *rdxA* gene would be expected to be associated with the development of resistance to Mtz. However, a number of Mtz-resistant strains have been reported in which the RdxA protein appears to be unchanged (23, 45, 49). In addition, Masaoka *et al.* has also isolated Mtz-resistant strains with an intact RdxA protein (31). These reports strongly suggest the existence of a resistance mechanism in the organisms other than RdxA inactivation. In the Mtz-resistant strains, superoxide radicals are generated through the reduction of Mtz; therefore, we focused on the radical scavenging activity in these Mtz-resistant strains.

*H. pylori* expresses only a single superoxide dismutase (SOD), the iron-cofactored superoxide dismutase (SodB) protein, which exhibits 53.5% identity to the *Escherichia coli* FeSod (41). SodB, as the primary defense against superoxide radicals, prevents interaction between iron and superoxide as

<sup>1</sup>Division of Gastroenterology and Hepatology, Department of Internal Medicine, Keio University School of Medicine, Tokyo, Japan.

<sup>2</sup>Department of Anatomy, School of Medicine, Showa University, Tokyo, Japan.

<sup>3</sup>Department of Biochemistry and Integrative Medical Biology, Keio University School of Medicine, Tokyo, Japan.

well as catalyzes the dismutation of superoxide into oxygen and hydrogen peroxide. In addition, expression of SodB is also essential for gastric colonization by *H. pylori* and for its growth under microaerobic conditions (40).

Recently, Ernst *et al.* reported that *sodB* expression in *H. pylori* is directly regulated by the ferric uptake regulator (Fur) protein. Fur functions as a global transcriptional regulator and is involved in acid tolerance, detoxification of reactive oxygen species (ROS), and energy metabolism in *H. pylori* (5, 7, 12, 29). It is reported that Fur binds to iron ( $\text{Fe}^{2+}$ ) and that the genes for iron uptake are repressed by the iron-binding form of Fur (10, 48). On the other hand, *sodB* expression is known to be repressed by the iron-free form of Fur (apo-Fur) (13). Apo-Fur binds to a specific consensus sequence called the Fur-Box located on the *sodB* promoter and blocks the binding of RNA polymerase (2, 13, 46).

In the present study, we attempted to confirm the hypothesis that Mtz-resistant strains which show no evident change of the RdxA protein exhibit an enhanced ability to defend themselves against superoxide radicals by SodB. The present study was designed to examine the expression of SodB and the structure and functions of Fur, which acts as a *sodB* transcriptional repressor, in Mtz-resistant strains.

## Materials and Methods

### Bacterial strains and culture conditions

*H. pylori* strains ATCC700392, KS0163, and KS0189 were used as the Mtz-susceptible strains; and strains KS0033, KS0048, and KS0145 were used as the Mtz-resistant strains. None of these Mtz-resistant strains showed any evident changes of the RdxA protein as determined by amino acid alignment analysis of the RdxA protein (31). According to the report of Masaoka *et al.*, KS0033 and KS0048 showed a moderate-level resistance ( $16 \leq$  minimum inhibitory concentration [MIC]  $< 32 \mu\text{g}/\text{mL}$ ), and KS0145 showed a high-level resistance ( $32 \mu\text{g}/\text{mL} \leq$  MIC) to Mtz (31). In this study, KS strains isolated from patients were maintained at  $-80^\circ\text{C}$  in Brucella Broth (Becton-Dickinson) containing 25% (vol/vol) glycerol. The bacteria were cultured on Columbia HP agar (Becton-Dickinson) for 2 days at  $37^\circ\text{C}$ , under microaerobic conditions maintained with AnaeroPack MicroAero (Mitsubishi).

### Total RNA isolation and quantitative RT-polymerase chain reaction

Since Fur activity is dependent on the concentration of iron in the medium, the bacteria, normalized to an  $\text{OD}_{600}$  of 0.5, were incubated with 0, 0.01 and  $0.05 \mu\text{g}/\text{mL}$  Mtz for 3 h in an iron-free medium (saline). The total RNA of the bacteria incubated with Mtz (Sigma) was isolated using the SV Total RNA Isolation system (Promega). The reverse transcription (RT) reaction was performed using the PrimeScript RT reagent Kit (Takara), in accordance with the manufacturer's guidelines. For real-time polymerase chain reaction (PCR), the PCR amplification was performed using the SYBR Premix Ex Taq Perfect Real Time kit (Takara) in a Thermal Cycler Dice Real Time System (Takara). The primer sequences used were as follows: *sodB* mRNA: forward 5'-CGACTGCCCTAAGC GATG and reverse 5'-CCAATTCCAACCAGAGCC; the 16S rRNA gene mRNA primers have been previously described in detail (35). The *H. pylori* 16S rRNA gene was used as the internal control for the quantitative RT-PCR.

### Measurement of SOD activity

Since the Fur activity is dependent on the concentration of iron in the medium, the bacteria, normalized to an  $\text{OD}_{600}$  of 0.5, were incubated with 0, 0.05, and  $0.5 \mu\text{g}/\text{mL}$  Mtz for 5 h in an iron-free medium (saline). After sonication (1.5 min at 25% power) of the bacteria incubated with Mtz, the resultant bacterial lysates were centrifuged, and the SOD activities were measured using an SOD Assay Kit-WST (Dojindo), in accordance with the manufacturer's guidelines.

### Electron spin resonance assay

A spin trapping agent,  $5 \mu\text{M}$  4-Hydroxy-TEMPO (Sigma) or 40 mM CYPMPO (Radical Research), was added to the bacteria, normalized to an  $\text{OD}_{600}$  of 0.5, and incubated with 0, 0.05 or  $0.5 \mu\text{g}/\text{mL}$  Mtz for 5 h. After sonication of the bacteria, the resultant bacterial lysates were transferred to a quartz flat cell (disposables) (Radical Research), and the radical intensity was determined by electron spin resonance (ESR) spectroscopy (JESRE1X, X-band; 100 kHz modulation frequency; Jeol) at  $20^\circ\text{C}$ .

### Measurement of RdxA activity

After sonication (1.5 min at 25% power) of the bacteria cultivated for 2 days in the Brucella Broth plate, the resultant bacterial lysates were centrifuged, and the protein concentrations were measured using the BCA method (Pierce). RdxA activity was spectrophotometrically measured with reduction of Mtz observed at 320 nm. The reaction mixture contained Tris/acetate (100 mM Tris-HCl, 50 mM acetate), pH 7.0, 0.05 mM Mtz, and 0.3 mM nicotine adenine dinucleotide (reduced form), as described by Goodwin *et al.* (14).

### Construction of SodB overexpression strain and rdxA deletion mutant strain

The shuttle vector pHel3 (19) was used as a scaffold to construct a SodB-overexpressing strain of *H. pylori*. The *sodB* gene was PCR-amplified with specific primers (forward 5'-CTCGAGATTAACCTTTTAAAAAATTTAAAAAGAATTTG and reverse 5'-GGTACCTTAAGCTTTTTTATGCACC) and cloned into the pHel3 shuttle vector as a *KpnI-XhoI* fragment. A nucleic acids sequencing of a *KpnI-XhoI* fragment was performed on the pHelSodB construct, and then the construct was electroporated into *H. pylori*, which was grown on kanamycin to obtain a SodB-overexpressing strain. On the other hand, *H. pylori* transfected with only the pHel3 shuttle vector was grown on kanamycin to obtain the control strain.

The target-region gene cassette (5'*rdxA*-chloramphenicol acetyltransferase (*cat*)-3'*rdxA*) for construction of *rdxA* deletion mutant strain was cloned into the pCR4-TOPO vector (Invitrogen, Carlsbad, CA), and then the sequences were determined (target-vector). The target-vector was electroporated into *H. pylori* ATCC700392, which was grown on 20  $\mu\text{g}$  chloramphenicol (Sigma) to obtain an *rdxA* deletion mutant strain of *H. pylori* ATCC700392.

### Measurement of the MIC to Mtz

The bacteria (at an  $\text{OD}_{600}$  of 0.1) were inoculated on an agar plate containing Mtz in serial twofold dilutions (0.5–128  $\mu\text{g}/\text{mL}$ ). All the plates were incubated at  $37^\circ\text{C}$  under microaerobic conditions, and the MIC values were determined (32).

### DNA sequencing and protein modeling of *H. pylori* Fur

The complete *fur* gene and the promoter region of *sodB* were PCR-amplified with specific primers (*fur* gene: forward 5'-ATGAAAAGATTAGAAAACCTTTC and reverse 5'-ACATTCACTCTCTGGCATTCT; *sodB* promoter gene: forward 5'-CCCTTAAAATCCACAAAATTTC and reverse 5'-GTAATGTAACATGTTTTCTCCTTG) using Ex Taq DNA polymerase (Takara). The PCR products were cloned into the pCR4-TOPO vector (Invitrogen), and then the sequences of the *fur* and *sodB* promoter genes were determined using the BigDye terminator V1.1 Cycle Sequencing Kit (Applied Biosystems); the deduced amino acids were then aligned using GENETYX Version 5.1. The protein structures were modeled and displayed using Swiss-Model ([www.expasy.org/swissmod](http://www.expasy.org/swissmod)) and DeepView-Swiss-PdbViewer ([www.expasy.org/spdbv/](http://www.expasy.org/spdbv/)), respectively.

### Expression and purification of *H. pylori* Fur

The *fur* gene was PCR-amplified with specific primers (ExFur gene: forward 5'-CATATGAAAAGATTAGAAAACCTTTC and reverse 5'-AGATCTGGACATTCACCTCTTTC) and cloned into the pET-30b (+) (Novagen) as an *NdeI*-*BglIII* fragment. The pETFur construct was transformed into *E. coli* BL21 (DE3), and the expression was achieved by induction, by the addition of 0.5 mM IPTG, of a 200 mL culture incubated for 6–8 h at 30°C and grown to an OD<sub>600</sub> of 0.6. The Fur protein expressed in this strain as a C-terminal Six-His tagged protein was purified using the MagneHis Protein Purification System (Promega).

### Apo-Fur binding analysis by surface plasmon resonance assay

A Biacore 2000 instrument (Biacore AB) was used to perform the Surface Plasmon Resonance assay in accordance with the manufacturer's guidelines. To construct the biotinylated *sodB* promoter gene of each strain, each *sodB* promoter

gene was PCR-amplified with specific biotinylated primers (forward 5'-CCCTTAAAATCCACAAAATTTC and reverse 5'-Bio-GTAATGTAACATGTTTTCTCCTTG). To conduct the analyses under a low-iron condition, the following buffer was used for the analyses: HBS-EP running buffer (10 mM HEPES, pH 7.4, 150 mM NaCl, 3 mM ethylenediaminetetraacetic acid, 0.005% surfactant P20) and biotinylated PCR products of the *sodB* promoter were immobilized on to Sensor Chip SA (GE Healthcare). At least five concentrations of each purified Fur protein were applied to the *sodB* promoter-immobilized Sensor Chip SA in HBS-EP buffer at a flow rate of 10  $\mu$ L/min. The response value of the reference cell (flow cell 3, blank) was subtracted from the response value of each flow cell 4 (*sodB* promoter) to correct for nonspecific binding. The data were analyzed, and the dissociation constant (*K<sub>d</sub>*) values were calculated using a BIAevaluation software (Biacore).

## Results

### Expression of SodB under Mtz exposure

In the Mtz-susceptible strain ATCC700392, *sodB* mRNA expression was scarcely derepressed under Mtz exposure (Fig. 1a). On the other hand, in the Mtz-resistant strains, which showed no evident change of the RdxA protein (KS0033, KS0048, and KS0145), the *sodB* mRNA expression was derepressed in a dose-dependent manner under exposure to Mtz (Fig. 1a). Further, no increase of the SodB activity was observed in the Mtz-susceptible strain, whereas significant increase of the SodB activity was found in the Mtz-resistant strains in the presence of 0.5  $\mu$ g/mL Mtz (Fig. 1b).

### Generation of superoxide radicals in *H. pylori* under Mtz exposure

To assess whether ROS generation was suppressed by the overexpression of SodB in the Mtz-resistant strains, we measured the amount of ROS produced in each type of *H. pylori*

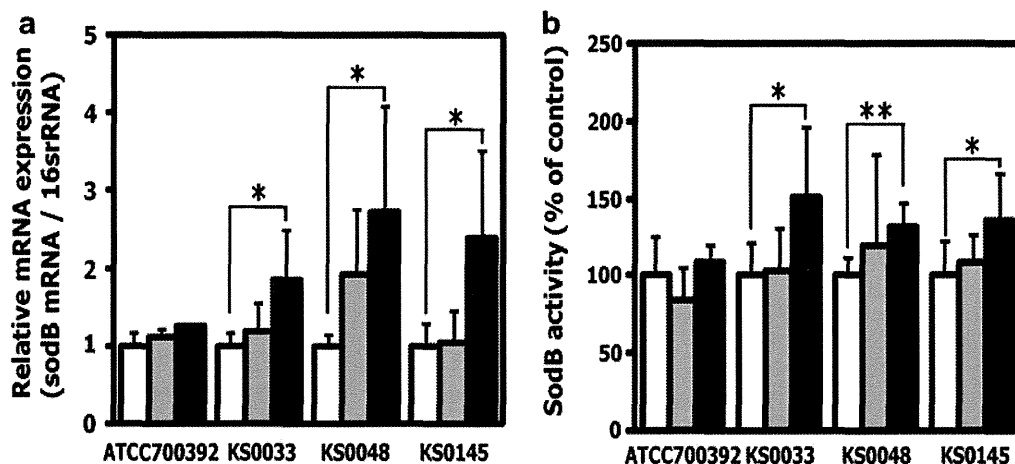


**FIG. 1. Expression of SodB under Mtz exposure.** (a) Expression of *sodB* mRNA in an Mtz-susceptible strain (ATCC700392) and Mtz-resistant strains (KS0033, KS0048, and KS0145) exposed to 0 (white), 0.01 (gray), and 0.05 (black)  $\mu$ g/mL Mtz was measured by quantitative reverse transcription–polymerase chain reaction. (b) Expression of SodB activity in an Mtz-susceptible strain (ATCC700392) and Mtz-resistant strains (KS0033, KS0048, and KS0145) exposed to 0 (white), 0.05 (gray), and 0.5 (black)  $\mu$ g/mL Mtz was measured by the method described in the Materials and Methods section. Results are means  $\pm$  SD of three independent assays. Asterisks indicate statistical significance from each strain with no Mtz exposure, \* $p < 0.05$ , \*\* $p < 0.01$ . Mtz, metronidazole; SodB, iron-cofactored superoxide dismutase.

strain under Mtz exposure by ESR assay. Although significant dose-dependent increase in the generation of ROS was observed after exposure to Mtz in the Mtz-susceptible strains, the ROS generation was significantly reduced in the Mtz-resistant strains (Fig. 2a). Further, Figure 2b shows the presence of the superoxide radical-specific signal of ESR detected with the CYPMPO reagent in the Mtz-susceptible strain, whereas no such specific signals can be seen in the Mtz-resistant strains.

#### Effect of SodB overexpression on *H. pylori* susceptibility to Mtz

To assess the contribution of the SodB overexpression to Mtz resistance, a SodB-overexpressing strain was constructed using a pHel3 shuttle vector (19). The SodB activity of the SodB-overexpressing strain (ATCC700392 pHel3::sodB) was twofold higher as compared with that of the control strain (ATCC700392 pHel3 control) (data not shown). Although the MIC of Mtz for the ATCC700392 strain and pHel3 control strain was the same as that for the Mtz-susceptible strains (MIC <8  $\mu\text{g}/\text{mL}$ ), the MIC values for KS0033, KS0048, KS0145, and ATCC700392 pHel3::sodB were 64, 32, 128, and 32  $\mu\text{g}/\text{mL}$ , respectively (Table 1). Thus, these strains showed a high level resistance to Mtz (MIC  $\geq 32 \mu\text{g}/\text{mL}$ ). In addition, to assess the Mtz reduction activity associated with Mtz resistance of KS0033, KS0048, and KS0145, the RdxA activity was spectrophotometrically measured with reduction of Mtz at 320 nm. The RdxA activity for KS0033, KS0048, KS0145, ATCC700392 pHel3::sodB, and ATCC700392 pHel3 control were not decreased compared with ATCC700392 (Table 1). On the other hand, the RdxA activity of ATCC700392  $\Delta\text{rdxA}$ , which showed a moderate-level resistance to Mtz (8  $\leq$  MIC <32  $\mu\text{g}/\text{mL}$ ), was significantly decreased compared with ATCC700392 (Table 1). This result indicated that RdxA inactivation did not contribute to development of the Mtz resistance in the KS0033, KS0048, KS0145, and ATCC700392

pHel3::sodB. Therefore, these findings strongly suggest that SodB overexpression contributes to Mtz resistance in the KS0033, KS0048, KS0145, and ATCC700392 pHel3::sodB.

#### Alignment of the nucleic acid sequence of the SodB promoter and the amino acid sequence of Fur

To assess the mechanism of SodB overexpression in the Mtz-resistant strains, we focused on the regulation of sodB expression by Fur. We aligned the nucleic acid sequence of the sodB promoter (Fur-Box) and the predicted amino acid sequence of Fur for the Mtz-susceptible strains (ATCC700392, KS0163, and KS0189) and Mtz-resistant strains (KS0033, KS0048, and KS0145). The A-5C mutation of the Fur-Box was detected in all of the clinical isolates from Keio University hospital (Fig. 3a). Although KS0145 showed a G-3A mutation adjacent to the Fur-Box, no distinct mutation of the Fur-Box was observed in the Mtz-resistant strains (Fig. 3a). On the other hand, two distinct mutations of the amino acid sequence of Fur were noted in the Mtz-resistant strains (Fig. 3b). KS0145 had a mutant-type Fur protein, with Cys 78 replaced by Tyr (C78Y) and Asn 118 replaced by His (N118H). KS0033 and KS0048 also showed a mutant-type of Fur, with Pro 114 replaced by Ser (P114S) and N118H (Fig. 3b). The HHDHXXCXXC motif, which is believed to be involved in the binding of the iron cofactor, was highly conserved (Fig. 3b) (4).

#### Kd value of apo-wild-type Fur and apo-mutant-type Fur

To assess the effect of the amino acid mutations of Fur (mutant-type Fur) on the affinity of apo-Fur for the Fur-Box, we examined the affinity of each of the apo-Fur proteins for the sodB promoter (Fur-Box) by Surface Plasmon Resonance assay (Biacore 2000). Beforehand, it was confirmed that the Kd value of apo-wild type (WT)-Fur to Fur-Box was similar to the value that Ernst *et al.* reported (13), and then the Kd value of

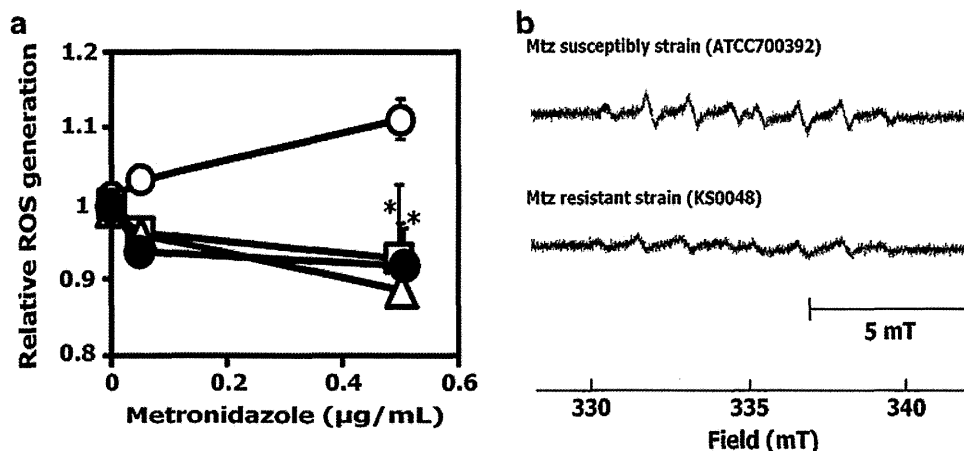


**FIG. 2. Generation of superoxide radicals under Mtz exposure.** (a) The induction of ROS was measured by electron spin resonance using 5  $\mu\text{M}$  4-Hydroxy-TEMPO in an Mtz-susceptible strain (ATCC700392) (white circle) and Mtz-resistant strains (KS0033 [white square], KS0048 [black circle], and KS0145 [white triangle]) exposed to 0, 0.05, and 0.5  $\mu\text{g}/\text{mL}$  Mtz. The ROS generation was calculated as reference in the ROS generation of each strain without Mtz exposure. Results are means  $\pm$  SD of three independent assays. Asterisks of KS0048 and KS0145 indicate statistical significance for the comparison with Mtz-susceptible strain (ATCC700392) as determined by Student's *t*-test ( $*p < 0.05$ ). (b) Representative signal patterns of generation of superoxide radicals in the Mtz-susceptible strain and Mtz-resistant strains exposed to 0.5  $\mu\text{g}/\text{mL}$  Mtz as measured by electron spin resonance using 40 mM CYPMPO. ROS, reactive oxygen species.

TABLE 1. THE EFFECT OF SUPEROXIDE DISMUTASE-OVEREXPRESSION AND RdxA ACTIVITY ON MINIMUM INHIBITORY CONCENTRATION ( $\mu\text{g}/\text{mL}$ ) OF METRONIDAZOLE

Strains	RdxA activity (nmol/min/mg protein)	p-Value	Minimum inhibitory concentration ( $\mu\text{g}/\text{mL}$ )	Metronidazole susceptibility
ATCC700392	2.57 $\pm$ 0.26		2	Susceptible level
ATCC700392 $\Delta rdxA$	1.29 $\pm$ 0.19	<0.01	16	Moderate level resistance
KS0033	2.45 $\pm$ 0.41	0.59	64	High level resistance
KS0048	2.35 $\pm$ 0.08	0.11	32	High level resistance
KS0145	2.40 $\pm$ 0.23	0.23	128	High level resistance
ATCC700392 pHel3::sodB	2.39 $\pm$ 0.05	0.16	32	High level resistance
ATCC700392 pHel3 control	2.77 $\pm$ 0.05	0.23	4	Susceptible level

SodB, iron-cofactored superoxide dismutase; RdxA, nicotinamide adenine dinucleotide phosphate (reduced form) nitroreductase.

apo-mutant-type Fur to Fur-Box as control with that of apo-WT-Fur was measured. The results of the assay revealed a significant increase of the  $K_d$  value for the apo-mutant-type Fur in the Mtz-resistant strains as compared with that of apo-WT-Fur in the Mtz-susceptible strains (Fig. 4). These results indicate a significantly decreased affinity of apo-mutant-type

Fur for the Fur-Box and that the SodB expression in the Mtz-resistant strains is not repressed to the same extent as that in the Mtz-susceptible strains (Fig. 5).

Further, to assess the effect of nucleic acid mutations of the *sodB* promoter on the affinity of apo-Fur for the Fur-Box, we examined the affinity of apo-ATCC700392 Fur for the KS0145

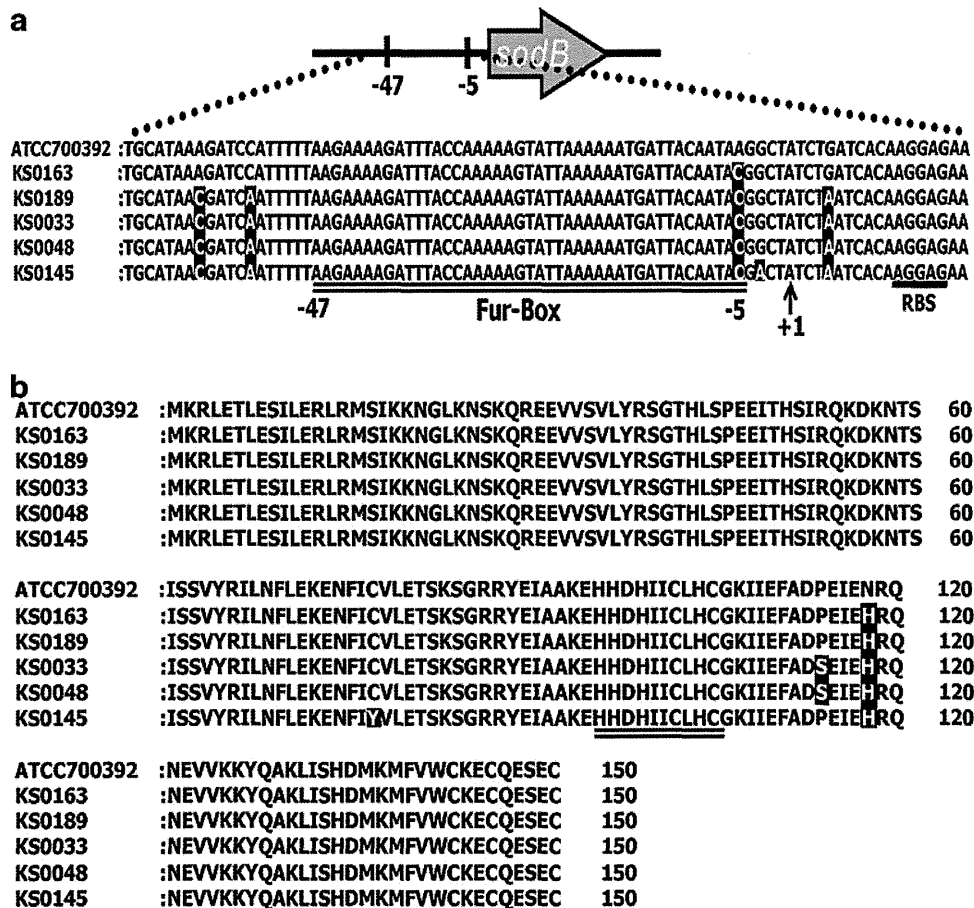
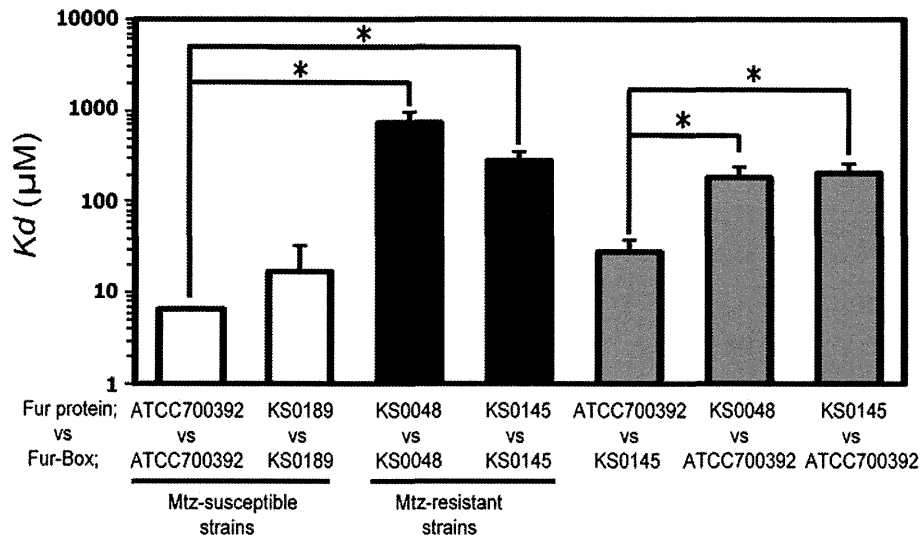


FIG. 3. Alignments of the *Helicobacter pylori* *sodB* promoter and Fur protein. (a) Alignment of the *sodB* promoter from the Mtz-susceptible strains (ATCC700392, KS0163, and KS0189) and Mtz-resistant strains (KS0033, KS0048, and KS0145). Each mutation point is marked in white. The predicted Fur-Box ranges from -5 to -47 and is indicated by the double line. +1 indicates the *sodB* transcriptional start site, and RBS indicates the ribosomal binding site. (b) Alignment of the predicted Fur amino acid sequences of Mtz-susceptible strains (ATCC700392, KS0163, and KS0189) and Mtz-resistant strains (KS0033, KS0048, and KS0145). Each mutation point is marked in white. The highly conserved motif (HHDXCXXC) believed to be involved in the binding of the iron cofactor is indicated by the double lines. Fur, ferric uptake regulator.





**FIG. 4. Mutation of Fur affects its affinity for the Fur-Box.** The  $K_d$  value for binding of each apo-Fur protein to each Fur-Box was calculated as reference in the Flow Cell in which *sodB* promoter was not immobilized on to Sensor Chip SA using a BIAevaluation software, and the combination of apo-Fur protein and Fur-Box is denoted as Fur protein *versus* Fur-Box. White bar indicates the affinity of apo-wild type (WT)-Fur for the Fur-Box of the Mtz-susceptible strains, black bar indicates the affinity of apo-mutant-type Fur for the Fur-Box in the Mtz-resistant strains, and the gray bar indicates the effect of the nucleic acid mutations of the Fur-Box on the affinity of apo-Fur for the Fur-Box. Results are means  $\pm$  SD of three independent assays. Asterisks indicate statistical significance from using an apo-WT-Fur,  $*p < 0.05$ .  $K_d$ , dissociation constant.

Fur-Box and the affinity of apo-mutant-type Fur for the ATCC700392 Fur-Box. The  $K_d$  value of apo-ATCC700392 Fur for binding to the KS0145 Fur-Box was fourfold higher as compared with that for the binding to the ATCC700392 Fur-Box, although the difference was not significant (Fig. 4). On the other hand, the  $K_d$  values of apo-mutant-type Fur for binding to the ATCC700392 Fur-Box were scarcely reduced as compared with that for its binding to the KS0145 or KS0048 Fur-Box (Fig. 4). The results of the assay revealed a significant increase of the  $K_d$  values of apo-mutant-type Fur for binding to the ATCC700392 Fur-Box as compared with that of apo-ATCC700392 Fur for binding to the KS0145 Fur-Box (Fig. 4).

#### Prediction of the three-dimensional structure of *H. pylori* Fur

To predict the positions of the mutations in the three-dimensional structure of Fur, the structure was determined using a Swiss Model and DeepView-Swiss-PdbViewer. The N-terminal domain possessing four helices followed by a loop was formed by the residues located between two antiparallel  $\beta$ -strands. The C-terminal domain, which was separated by a coil from the N-terminus possessing two antiparallel  $\beta$ -strands, was followed by another  $\beta$ -strand located between the two helices (Fig. 6). C78Y is predicted to belong to a  $\beta$  strand in the N-terminal domain, whereas P114S and N118H are predicted to belong to a C-terminal domain (Fig. 6).

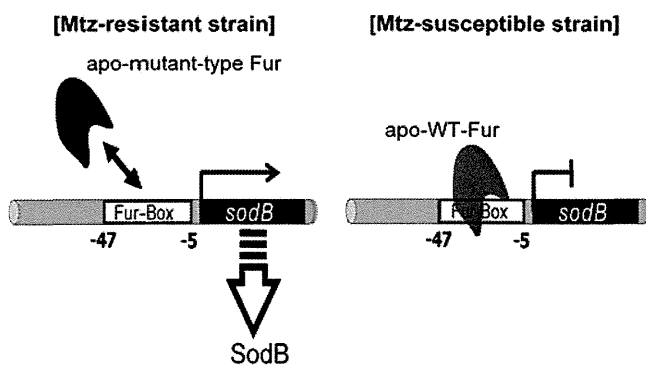


**FIG. 5. Schematic representation of the proposed mode of action of apo-mutant type-Fur in the Mtz-resistant strains and apo-WT-Fur in the Mtz-susceptible strains.** The apo-Fur binds to an operator sequence called Fur-Box in the *sodB* promoter, and then binding of apo-Fur suppresses *sodB* expression. The affinity of the apo-mutant-type Fur to the Fur-Box is significantly decreased, and then *sodB* expression of Mtz-resistant strains is more derepressed than Mtz-susceptible strains.

#### Discussion

The present study revealed amino acid mutations of Fur in some Mtz-resistant strains with the RdxA activity remaining with reduced affinity of the mutant Fur for the Fur-Box, and enhancement of the superoxide radical scavenging activity in these strains, as *sodB* was not repressed to the same extent by the apo-mutant-type Fur in these strains as by the wild-type apo-fur in the Mtz-susceptible strains (Figs. 1–4, Table 1).

Recently, Carpenter *et al.* reported that the A-5C mutation of the Fur-Box decreases the affinity of apo-Fur for the Fur-Box in *H. pylori* (6). In the present study, the A-5C mutation of the Fur-Box was detected in all of the tested clinical isolates (Fig. 3a). In the Surface Plasmon Resonance assay, the  $K_d$  value for the binding of apo-ATCC700392 Fur to the KS0145 Fur-Box was fourfold higher as compared with that for its binding to the ATCC700392 Fur-Box (Fig. 4), suggesting that the A-5C mutation in the Fur-Box is important for the binding with apo-ATCC700392 Fur, which is consistent with the report of Carpenter *et al.* (6). On the other hand, in the Mtz-resistant strains, the A-5C mutation hardly influenced the interaction between



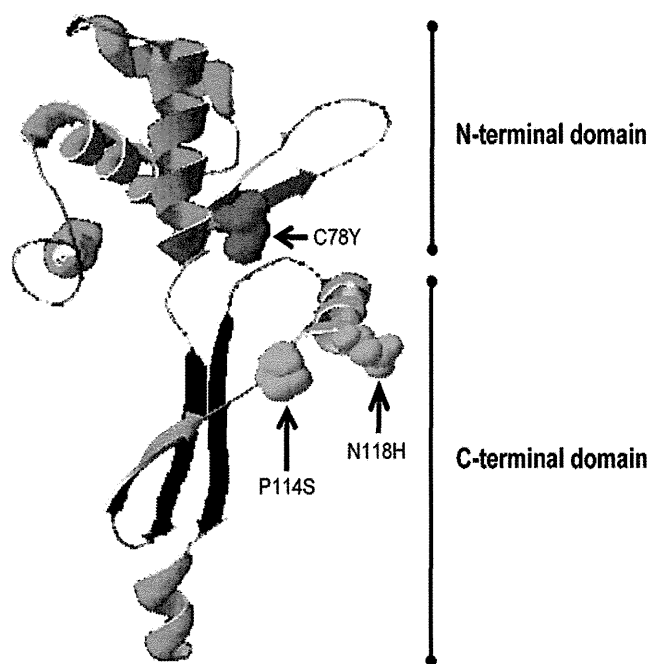


**FIG. 6. Prediction of the three-dimensional structure of the Fur protein.** Each mutation point is marked with an arrow. C78Y is predicted to exist in the N-terminal domain, whereas P114S and N118H are predicted to be located in the C-terminal domain. The three-dimensional structure was determined using a Swiss-Model and DeepView-Swiss-PdbViewer. (For interpretation of the references to color in this figure legend, the reader is referred to the web version of this article at [www.liebertonline.com/ars](http://www.liebertonline.com/ars)).

the Fur-Box and the apo-mutant-type Fur (Fig. 4). These results indicate that the Fur mutations C78Y, P114S, and N118H could play a greater role on the affinity of apo-Fur for the Fur-Box than the A-5C mutation in the Fur-Box.

The Fur protein has been best characterized in *E. coli*, in which it has been shown to possess three functional domains (the DNA-binding domain, iron-binding domain, and the oligomerization domain), and the protein binds to the Fur-Box after dimerization (17, 36, 42, 46). The Fur monomer of *E. coli* has been reported to consist of a helix-turn-helix motif and two  $\beta$  strands separated by a turn that forms the wings on the N-terminal domain, which is considered to be involved in the DNA binding (21, 42, 46). On the other hand, the C-terminal domain of *E. coli* Fur, separated by a coil from the N-terminal, consists of two antiparallel  $\beta$ -strands, which are considered to be involved in the oligomerization of the protein (21, 42). From the results of the homology modeling of *H. pylori* Fur, it was inferred that *H. pylori* Fur also has three functional domains (the DNA-binding domain near the N-terminal, iron cofactor-binding domain (HHDHXXCXXC), and the oligomerization domain near the C-terminal) (4). Therefore, it was inferred that the C78Y mutation of the KS0145 strain was located in the DNA-binding domain and that the P114S and N118H mutations of KS0033 and KS0048 strains were located in the oligomerization domain using a homology modeling (Fig. 6). Therefore, these mutations are predicted to affect the affinity of the Fur protein for the Fur-Box. However, the amino acid sequence of *H. pylori* Fur exhibited moderate identity (23%–37%) to the Fur protein from other bacteria

present in the database, such as *Campylobacter jejuni*, *E. coli*, *Haemophilus influenzae*, *Vibrio cholerae*, *Bordetella pertussis*, *Klebsiella pneumoniae*, *Neisseria meningitidis*, *Staphylococcus epidermidis*, *Pseudomonas aeruginosa*, and *Bacillus subtilis*, suggestive of a moderate homology (4). This finding indicates that the amino acids which are important for DNA binding or dimerization may differ between *H. pylori* Fur and other bacterial Fur proteins.

ROS damage of pathogenic bacteria constitutes a key part of the immune response of the host. Many studies have shown that *H. pylori* infection elicits a strong oxidative stress response from the host (1, 3, 9, 44). To survive the effects of production of ROS by the host, *H. pylori* depends on a significant repertoire of detoxification enzymes, such as SodB, catalase (KatA), and neutrophil-activating protein (NapA) (18, 34, 41). Upstream of *katA*, a low-affinity putative Fur-Box has been identified (30, 33). In addition, Cooksley *et al.* reported that Fur is involved in *napA* regulation and that a potential Fur-Box by which this control could be mediated has been identified (8). Accordingly, the expression of *katA* and/or *napA* might be derepressed by mutant-type Fur, leading to enhancement of the ability of *H. pylori* to colonize the human stomach.

In the present study, we demonstrated that the overexpression of SodB mediated by mutant-type Fur may underlie the RdxA-independent resistance of *H. pylori* to Mtz. Recently, it has come to be recognized that in addition to RdxA, some other proteins such as pyruvate oxidoreductase, nicotinamide adenine dinucleotide phosphate (reduced form) flavin oxidoreductase (FrxA), and ferredoxin-like protein (FdxB) may also be associated with the activation of Mtz (22, 25). Many researchers have demonstrated an association between inactivation of these proteins and resistance to Mtz (20, 24, 27, 28). On the other hand, Jenks *et al.* reported that RdxA-independent mechanisms may play only a relatively minor role in Mtz resistance or may be involved only in the transition to high-level resistance (22). Although it is difficult to determine whether overexpression of SodB associated with mutant-type Fur entirely accounts for RdxA-independent Mtz resistance, it is, nevertheless, an important mechanism that participates in not only Mtz resistance but also resistance of the host immune responses to ROS.

Recently, overexpression of Fe-SOD was reported to be associated with the Mtz resistance in Mtz-resistant strains of the protozoan parasite *Entamoeba histolytica*, which is the causative agent of human amoebiasis (39, 50). Based on these reports, it is considered that overexpression of SOD may affect the Mtz resistance mechanism in many bacterial species.

In conclusion, the present study demonstrates a novel mechanism of Mtz resistance of *H. pylori*, namely, aberrant increase of SodB expression resulting from mutations of Fur.

#### Acknowledgments

The authors are grateful to Dr. Rainer Haas of Ludwig-Maximilians-University, Munich, for providing us the pHel shuttle vectors.

This work was supported by a Grant-in-Aid for Young Scientists (B) from the Japan Society for the Promotion of Science (21790133, to H.T.), a Grant-in-Aid for Scientific Research (B) from the Japan Society for the Promotion of Science (22300169, to H.S.), a grant from the Smoking Research Foundation (to H.S.), Keio Gijuku Academic Development

Funds (to H.S.), and Keio University Research grants for Life Sciences and Medicine (99-095-0009, to H.T.).

This work was awarded the Prize for Best Investigator at the 18th Digestive and Free Radical Workshop, the Young Investigator Award at the 62nd Society for Free Radical Research Japan, and also the Uehara *H. pylori* Award at the 15th Japanese Society for Helicobacter Research. A part of this work was presented at a Research Forum in Digestive Disease Week 2009 in Chicago, IL.

#### Author Disclosure Statement

No competing financial interests exist.

#### References

- Allen LA. Phagocytosis and persistence of *Helicobacter pylori*. *Cell Microbiol* 9: 817–828, 2007.
- Baichoo N and Helmann JD. Recognition of DNA by Fur: a reinterpretation of the Fur box consensus sequence. *J Bacteriol* 184: 5826–5832, 2002.
- Baik SC, Youn HS, Chung MH, Lee WK, Cho MJ, Ko GH, Park CK, Kasai H, and Rhee KH. Increased oxidative DNA damage in *Helicobacter pylori*-infected human gastric mucosa. *Cancer Res* 56: 1279–1282, 1996.
- Bereswill S, Lichte F, Vey T, Fassbinder F, and Kist M. Cloning and characterization of the fur gene from *Helicobacter pylori*. *FEMS Microbiol Lett* 159: 193–200, 1998.
- Bijlsma JJ, Waidner B, Vliet AH, Hughes NJ, Hag S, Bereswill S, Kelly DJ, Vandenbroucke-Grauls CM, Kist M, and Kusters JG. The *Helicobacter pylori* homologue of the ferric uptake regulator is involved in acid resistance. *Infect Immun* 70: 606–611, 2002.
- Carpenter BM, Gancz H, Gonzalez-Nieves RP, West AL, Whitmire JM, Michel SL, and Merrell DS. A single nucleotide change affects fur-dependent regulation of *sodB* in *H. pylori*. *PLoS One* 4: e5369, 2009.
- Choi YW, Park SA, Lee HW, and Lee NG. Alteration of growth-phase-dependent protein regulation by a fur mutation in *Helicobacter pylori*. *FEMS Microbiol Lett* 294: 102–110, 2009.
- Cooksley C, Jenks PJ, Green A, Cockayne A, Logan RP, and Hardie KR. NapA protects *Helicobacter pylori* from oxidative stress damage, and its production is influenced by the ferric uptake regulator. *J Med Microbiol* 52: 461–469, 2003.
- Davies GR, Simmonds NJ, Stevens TR, Sheaff MT, Banatvala N, Laurenson IF, Blake DR, and Rampton DS. *Helicobacter pylori* stimulates antral mucosal reactive oxygen metabolite production *in vivo*. *Gut* 35: 179–185, 1994.
- Delany I, Pacheco AB, Spohn G, Rappuoli R, and Scarlato V. Iron-dependent transcription of the *frpB* gene of *Helicobacter pylori* is controlled by the Fur repressor protein. *J Bacteriol* 183: 4932–4937, 2001.
- Dunn BE, Cohen H, and Blaser MJ. *Helicobacter pylori*. *Clin Microbiol Rev* 10: 720–741, 1997.
- Ernst FD, Bereswill S, Waidner B, Stoof J, Mader U, Kusters JG, Kuipers EJ, Kist M, van Vliet AH, and Homuth G. Transcriptional profiling of *Helicobacter pylori* Fur- and iron-regulated gene expression. *Microbiology* 151: 533–546, 2005.
- Ernst FD, Homuth G, Stoof J, Mader U, Waidner B, Kuipers EJ, Kist M, Kusters JG, Bereswill S, and van Vliet AH. Iron-responsive regulation of the *Helicobacter pylori* iron-factored superoxide dismutase *SodB* is mediated by Fur. *J Bacteriol* 187: 3687–3692, 2005.
- Goodwin A, Kersulyte D, Sisson G, Veldhuyzen van Zanten SJ, Berg DE, and Hoffman PS. Metronidazole resistance in *Helicobacter pylori* is due to null mutations in a gene (*rdxA*) that encodes an oxygen-insensitive NADPH nitroreductase. *Mol Microbiol* 28: 383–393, 1998.
- Group EHPS. Current European concepts in the management of *Helicobacter pylori* infection. The Maastricht Consensus Report. *Gut* 41: 8–13, 1997.
- Group TES. An international association between *Helicobacter pylori* infection and gastric cancer. *Lancet* 341: 1359–1362, 1993.
- Hamed MY and Al-Jabour S. Iron(II) triggered conformational changes in *Escherichia coli* fur upon DNA binding: a study using molecular modeling. *J Mol Graph Model* 25: 234–246, 2006.
- Hazell SL, Evans DJ Jr., and Graham DY. *Helicobacter pylori* catalase. *J Gen Microbiol* 137: 57–61, 1991.
- Heuermann D and Haas R. A stable shuttle vector system for efficient genetic complementation of *Helicobacter pylori* strains by transformation and conjugation. *Mol Gen Genet* 257: 519–528, 1998.
- Hoffman PS, Goodwin A, Johnsen J, Magee K, and Veldhuyzen van Zanten SJ. Metabolic activities of metronidazole-sensitive and -resistant strains of *Helicobacter pylori*: repression of pyruvate oxidoreductase and expression of isocitrate lyase activity correlate with resistance. *J Bacteriol* 178: 4822–4829, 1996.
- Jabour S and Hamed MY. Binding of the Zn<sup>2+</sup> ion to ferric uptake regulation protein from *E. coli* and the competition with Fe<sup>2+</sup> binding: a molecular modeling study of the effect on DNA binding and conformational changes of Fur. *J Comput Aided Mol Des* 23: 199–208, 2009.
- Jenks PJ and Edwards DI. Metronidazole resistance in *Helicobacter pylori*. *Int J Antimicrob Agents* 19: 1–7, 2002.
- Jenks PJ, Ferrero RL, and Labigne A. The role of the *rdxA* gene in the evolution of metronidazole resistance in *Helicobacter pylori*. *J Antimicrob Chemother* 43: 753–758, 1999.
- Jeong JY, Mukhopadhyay AK, Dailidienė D, Wang Y, Velapattino B, Gilman RH, Parkinson AJ, Nair GB, Wong BC, Lam SK, Mistry R, Segal I, Yuan Y, Gao H, Alarcon T, Brea ML, Ito Y, Kersulyte D, Lee HK, Gong Y, Goodwin A, Hoffman PS, and Berg DE. Sequential inactivation of *rdxA* (HP0954) and *frxA* (HP0642) nitroreductase genes causes moderate and high-level metronidazole resistance in *Helicobacter pylori*. *J Bacteriol* 182: 5082–5090, 2000.
- Jorgensen MA, Trend MA, Hazell SL, and Mendz GL. Potential involvement of several nitroreductases in metronidazole resistance in *Helicobacter pylori*. *Arch Biochem Biophys* 392: 180–191, 2001.
- Kim JJ, Reddy R, Lee M, Kim JG, El-Zaatari FA, Osato MS, Graham DY, and Kwon DH. Analysis of metronidazole, clarithromycin and tetracycline resistance of *Helicobacter pylori* isolates from Korea. *J Antimicrob Chemother* 47: 459–461, 2001.
- Kwon DH, El-Zaatari FA, Kato M, Osato MS, Reddy R, Yamaoka Y, and Graham DY. Analysis of *rdxA* and involvement of additional genes encoding NAD(P)H flavin oxidoreductase (*FrxA*) and ferredoxin-like protein (*FdxB*) in metronidazole resistance of *Helicobacter pylori*. *Antimicrob Agents Chemother* 44: 2133–2142, 2000.
- Kwon DH, Kato M, El-Zaatari FA, Osato MS, and Graham DY. Frame-shift mutations in NAD(P)H flavin oxidoreductase encoding gene (*frxA*) from metronidazole resistant *Helicobacter pylori* ATCC43504 and its involvement in metronidazole resistance. *FEMS Microbiol Lett* 188: 197–202, 2000.

29. Lee HW, Choe YH, Kim DK, Jung SY, and Lee NG. Proteomic analysis of a ferric uptake regulator mutant of *Helicobacter pylori*: regulation of *Helicobacter pylori* gene expression by ferric uptake regulator and iron. *Proteomics* 4: 2014–2027, 2004.
30. Manos J, Kolesnikow T, and Hazell SL. An investigation of the molecular basis of the spontaneous occurrence of a catalase-negative phenotype in *Helicobacter pylori*. *Helicobacter* 3: 28–38, 1998.
31. Masaoka S, Suzuki H, Kurabayashi K, Nomoto Y, Nishizawa T, Mori M, and Hibi T. Could frameshift mutations in the *frxA* and *rdxA* genes of *Helicobacter pylori* be a marker for metronidazole resistance? *Aliment Pharmacol Ther* 24: 81–87, 2006.
32. Nagayama A, Yamaguchi K, Watanabe K, Tanaka M, Kobayashi I, and Nagasawa Z. Final report from the Committee on Antimicrobial Susceptibility Testing, Japanese Society of Chemotherapy, on the agar dilution method (2007). *J Infect Chemother* 14: 383–392, 2008.
33. Odenbreit S, Wieland B, and Haas R. Cloning and genetic characterization of *Helicobacter pylori* catalase and construction of a catalase-deficient mutant strain. *J Bacteriol* 178: 6960–6967, 1996.
34. Olczak AA, Wang G, and Maier RJ. Up-expression of NapA and other oxidative stress proteins is a compensatory response to loss of major *Helicobacter pylori* stress resistance factors. *Free Radic Res* 39: 1173–1182, 2005.
35. Osaki T, Hanawa T, Manzoku T, Fukuda M, Kawakami H, Suzuki H, Yamaguchi H, Yan X, Taguchi H, Kurata S, and Kamiya S. Mutation of *luxS* affects motility and infectivity of *Helicobacter pylori* in gastric mucosa of a Mongolian gerbil model. *J Med Microbiol* 55: 1477–1485, 2006.
36. Pecqueur L, D'Autreaux B, Dupuy J, Nicolet Y, Jacquamet L, Brutscher B, Michaud-Soret I, and Bersch B. Structural changes of *Escherichia coli* ferric uptake regulator during metal-dependent dimerization and activation explored by NMR and X-ray crystallography. *J Biol Chem* 281: 21286–21295, 2006.
37. Perez-Reyes E, Kalyanaraman B, and Mason RP. The reductive metabolism of metronidazole and ronidazole by aerobic liver microsomes. *Mol Pharmacol* 17: 239–244, 1980.
38. Rao DN and Mason RP. Generation of nitro radical anions of some 5-nitrofurans, 2- and 5-nitroimidazoles by norepinephrine, dopamine, and serotonin. A possible mechanism for neurotoxicity caused by nitroheterocyclic drugs. *J Biol Chem* 262: 11731–11736, 1987.
39. Samarawickrema NA, Brown DM, Upcroft JA, Thammappalerd N, and Upcroft P. Involvement of superoxide dismutase and pyruvate:ferredoxin oxidoreductase in mechanisms of metronidazole resistance in *Entamoeba histolytica*. *J Antimicrob Chemother* 40: 833–840, 1997.
40. Seyler RW Jr., Olson JW, and Maier RJ. Superoxide dismutase-deficient mutants of *Helicobacter pylori* are hypersensitive to oxidative stress and defective in host colonization. *Infect Immun* 69: 4034–4040, 2001.
41. Spiegelhalder C, Gerstenecker B, Kersten A, Schiltz E, and Kist M. Purification of *Helicobacter pylori* superoxide dismutase and cloning and sequencing of the gene. *Infect Immun* 61: 5315–5325, 1993.
42. Stojiljkovic I and Hantke K. Functional domains of the *Escherichia coli* ferric uptake regulator protein (Fur). *Mol Gen Genet* 247: 199–205, 1995.
43. Suzuki H, Hibi T, and Marshall BJ. *Helicobacter pylori*: present status and future prospects in Japan. *J Gastroenterol* 42: 1–15, 2007.
44. Suzuki H, Mori M, Seto K, Kai A, Kawaguchi C, Suzuki M, Suematsu M, Yoneta T, Miura S, and Ishii H. *Helicobacter pylori*-associated gastric pro- and antioxidant formation in Mongolian gerbils. *Free Radic Biol Med* 26: 679–684, 1999.
45. Tankovic J, Lamarque D, Delchier JC, Soussy CJ, Labigne A, and Jenks PJ. Frequent association between alteration of the *rdxA* gene and metronidazole resistance in French and North African isolates of *Helicobacter pylori*. *Antimicrob Agents Chemother* 44: 608–613, 2000.
46. Tiss A, Barre O, Michaud-Soret I, and Forest E. Characterization of the DNA-binding site in the ferric uptake regulator protein from *Escherichia coli* by UV crosslinking and mass spectrometry. *FEBS Lett* 579: 5454–5460, 2005.
47. van der Wouden EJ, van Zwet AA, Vosmaer GD, Oom JA, de Jong A, and Kleibeuker JH. Rapid increase in the prevalence of metronidazole-resistant *Helicobacter pylori* in the Netherlands. *Emerg Infect Dis* 3: 385–389, 1997.
48. van Vliet AH, Stoof J, Vlasblom R, Wainwright SA, Hughes NJ, Kelly DJ, Bereswill S, Bijlsma JJ, Hoogenboezem T, Vandenbroucke-Grauls CM, Kist M, Kuipers EJ, and Kusters JG. The role of the ferric uptake regulator (Fur) in regulation of *Helicobacter pylori* iron uptake. *Helicobacter* 7: 237–244, 2002.
49. Wang G, Wilson TJ, Jiang Q, and Taylor DE. Spontaneous mutations that confer antibiotic resistance in *Helicobacter pylori*. *Antimicrob Agents Chemother* 45: 727–733, 2001.
50. Wassmann C, Hellberg A, Tannich E, and Bruchhaus I. Metronidazole resistance in the protozoan parasite *Entamoeba histolytica* is associated with increased expression of iron-containing superoxide dismutase and peroxiredoxin and decreased expression of ferredoxin 1 and flavin reductase. *J Biol Chem* 274: 26051–26056, 1999.

Address correspondence to:

Dr. Hidekazu Suzuki

Division of Gastroenterology and Hepatology

Department of Internal Medicine

Keio University School of Medicine

35 Shinanomachi, Shinjuku-ku

Tokyo 160-8582

Japan

E-mail: hsuzuki@sc.itc.keio.ac.jp

Date of first submission to ARS Central, February 8, 2010; date of final revised submission, May 27, 2010; date of acceptance, June 2, 2010.

#### Abbreviations Used

ESR = electron spin resonance

Fur = ferric uptake regulator

$K_d$  = dissociation constant

Mtz = metronidazole

PCR = polymerase chain reaction

RdxA = nicotinamide adenine dinucleotide

phosphate (reduced form)

nitroreductase

ROS = reactive oxygen species

SodB = iron-cofactored superoxide dismutase

# BASIC—ALIMENTARY TRACT

## Dysfunctional Gastric Emptying With Down-regulation of Muscle-Specific MicroRNAs in *Helicobacter pylori*-Infected Mice

YOSHIMASA SAITO, HIDEKAZU SUZUKI, HITOSHI TSUGAWA, SACHIKO SUZUKI, JUNTARO MATSUZAKI, KENRO HIRATA, and TOSHIFUMI HIBI

Division of Gastroenterology and Hepatology, Department of Internal Medicine, Keio University School of Medicine, Shinjuku-ku, Tokyo, Japan

**BACKGROUND & AIMS:** Little is known about the pathogenic mechanisms of functional dyspepsia. We investigated the role of microRNAs (miRNAs) in gastric motility disorders associated with *Helicobacter pylori* infection. **METHODS:** Male C57BL/6 mice were infected with *H pylori*. After long-term infection, gastric emptying was examined and compared with that of uninfected mice (controls). The miRNA expression profile was analyzed by miRNA microarray and quantitative reverse-transcriptase polymerase chain reaction. The results obtained from the animal study were confirmed by in vitro experiments. **RESULTS:** Gastric emptying was significantly accelerated in mice after chronic infection with *H pylori*. Histologic examination showed that the muscular layers of the stomachs of *H pylori*-infected mice were significantly thickened. The miRNA expression profile revealed that the muscle-specific miRNAs *miR-1* and *miR-133* were significantly down-regulated in the stomachs after long-term infection with *H pylori*. However, expression of histone deacetylase 4 and serum response factor, which are reported target genes of *miR-1* and *miR-133*, increased. Down-regulation of *miR-1* and *miR-133* and increased cell proliferation were observed in C2C12 mouse myoblast cells after coculture with *H pylori*. **CONCLUSIONS:** Chronic infection with *H pylori* down-regulates expression of muscle-specific miRNAs and up-regulates expression of histone deacetylase 4 and serum response factor. These might cause hyperplasia in the muscular layer of the stomach and dysfunction in gastric emptying. These findings provide insight into the molecular pathogenesis of gastric motility disorders, including functional dyspepsia.

**Keywords:** Functional Gastrointestinal Disorder; Noncoding RNA; Muscle Cell; Liquid Gastric Emptying.

*Helicobacter pylori* has been shown to be involved not only in the pathogenesis of chronic gastritis, peptic ulcer, and gastric cancer<sup>1–5</sup> but also in gastric motility disorders such as functional dyspepsia (FD).<sup>6–8</sup> Although delayed gastric emptying has been reported in patients with FD,<sup>9–11</sup> several studies have failed to confirm such a

relationship.<sup>12,13</sup> Recent studies have shown that accelerated gastric emptying in patients with FD is associated with postprandial fullness, bloating, nausea, and stomach pain<sup>14</sup> and that gastric emptying is significantly accelerated in *H pylori*-positive children with nonulcer dyspepsia in comparison with noninfected children.<sup>15</sup> Lee et al<sup>16</sup> have reported that spontaneous duodenal acid exposure is increased in a subset of FD patients who are characterized with more severe dyspeptic symptoms. They suggested that increased duodenal acid may enhance the pathophysiology of FD, producing symptoms such as delayed gastric emptying. Despite many clinical studies of affected patients, the pathogenesis of FD is still poorly understood.

MicroRNAs (miRNAs) are small noncoding RNAs that function as endogenous silencers of target genes, thus playing critical roles in cell proliferation, apoptosis, and differentiation during mammalian development.<sup>17</sup> Links between miRNAs and human cancers are becoming increasingly apparent, and aberrant expression of miRNAs is known to be involved in the initiation and progression of gastrointestinal (GI) cancers.<sup>18–24</sup> Moreover, recent studies have revealed that *miR-29a* and *miR-510* are involved in the pathophysiology of irritable bowel syndrome (IBS), indicating that miRNAs play important roles not only in GI cancers but also in functional GI disorders such as IBS.<sup>25,26</sup> To investigate the molecular mechanism underlying the pathogenesis of functional gastric disorders associated with *H pylori* infection, we analyzed the miRNA expression profile in the stomachs of mice after long-term infection with *H pylori*.

**Abbreviations used in this paper:**  $\alpha$ -SMA,  $\alpha$ -smooth muscle actin; BrdU, bromodeoxyuridine; CFU, colony-forming unit; DAPI, 4',6-diamidino-2-phenylindole; ELISA, enzyme-linked immunosorbent assay; FD, functional dyspepsia; GI, gastrointestinal; HDAC4, histone deacetylase 4; *H pylori*, *Helicobacter pylori*; IBS, irritable bowel syndrome; IL, interleukin; miRNA, microRNA; RT-PCR, reverse-transcription polymerase chain reaction; SRF, serum response factor; TNF, tumor necrosis factor.

© 2011 by the AGA Institute  
0016-5085/\$36.00  
doi:10.1053/j.gastro.2010.08.044

In the present study, we found that gastric emptying was accelerated in *H pylori*-infected mice. Interestingly, the miRNA expression profile revealed that *miR-1* and *miR-133* were markedly down-regulated in the stomach after chronic infection with *H pylori*. It has been reported that *miR-1* and *miR-133* are highly expressed in differentiated muscle tissues and control muscle differentiation and proliferation.<sup>27,28</sup> In addition, it has been shown that the expression of *miR-1* and *miR-133* is decreased in mouse and human cardiac hypertrophy, thus playing an essential role in the development of heart disease.<sup>29-32</sup> Here, we present novel data that offer insights into the molecular pathogenesis of gastric motility disorder associated with chronic *H pylori* infection via aberrant expression of muscle-specific miRNAs.

## Materials and Methods

### Animals and *H pylori* Infection

All experiments and procedures in this study were approved by the Keio University Animal Research Committee. A total of 14 male C57BL/6 mice were infected with *H pylori* (the Sydney strain; SS1) at a concentration of  $10^6$  colony-forming units (CFUs)/mL by oral gavage. Fourteen uninfected male wild-type C57BL/6 mice were used as controls. After 40 weeks of infection, the mice with *H pylori* infection ( $n = 7$ ) and age-matched control mice ( $n = 7$ ) were killed, and then their stomachs were dissected out and subjected to histologic examination and extraction of RNA and protein. Gastric emptying of mice chronically infected with *H pylori* and *Helicobacter felis* (53 weeks after infection;  $n = 7$  and  $n = 13$ , respectively) and control mice ( $n = 7$ ) was evaluated as described below.

*Helicobacter* infection was confirmed in all the stomachs of *Helicobacter*-infected mice by microaerobic bacterial culture of stomach homogenates on Nissui Plate *Helicobacter* Agar (Nissui, Tokyo, Japan) and histologic examination.

### Evaluation of Gastric Emptying

Gastric emptying in mice was evaluated by measuring the amount of phenol red remaining in the stomach after oral administration. The experiment was conducted according to the method reported by Suzuki et al.<sup>33</sup> Each mouse received 200  $\mu$ L of phenol red (100  $\mu$ g/mL) orally and was killed 15 minutes later, except for some mice that were killed immediately after administration to recover the entire dose of phenol red. The stomach was removed immediately and washed in 10 mL of  $\text{Na}_2\text{HPO}_4$  solution (0.1 mol/L) to collect the gastric contents and phenol red, and then 1 mL of the rinse solution was added to 0.5 mL of  $\text{Na}_2\text{HPO}_4$  solution (0.1 mol/L) (S1: the rinse solution and  $\text{Na}_2\text{HPO}_4$  solution). The residual rinse solution was added to 1 mL of phenol red (100  $\mu$ g/mL) solution and then diluted 5-fold with

$\text{Na}_2\text{HPO}_4$  solution (0.1 mol/L) (S2: diluted solution of the residual rinse solution and phenol red). The absorbances of solutions S1 and S2 were measured at a wavelength of 570 nm with a microplate reader (Bio-Rad, Hercules, CA). Gastric emptying was calculated as follows:

$$\text{Gastric emptying}(\%) = 100 - (A/B) \times 100$$

A: Amount of phenol red remaining in the stomach (micrograms)

$$= (100 - [1.5 \times \langle S1 \rangle]) / (5 \times \langle S2 \rangle / [1.5 \times \langle S1 \rangle] - 1)$$

Note:  $\langle S1 \rangle$  and  $\langle S2 \rangle$  are the phenol red concentrations in solutions S1 and S2.

B: The amount of phenol red recovered from the stomach immediately after phenol red administration (micrograms).

### Histologic Examination

Tissues were stained with H&E and subjected to histologic examination. Thickness of smooth muscle was expressed as the averaged value of the thickness of the muscularis propria layer at 3 points in the corpus (oral side, middle, anal side) determined by microscopy ( $\times 40$ ) from comparison with a size scale.

4',6-Diamidino-2-phenylindole (DAPI) staining was performed, and the nuclei of myocytes were counted using the fluorescence microscope (Eclipse E600; Nikon Corporation, Tokyo, Japan). The average number of myocytes in the muscular layer in 2 randomly selected microscopic fields ( $\times 200$ ) was examined.

### RNA Extraction and Microarray Analysis

Total RNAs of tissue specimens from the stomachs of *H pylori*-infected mice and control mice were extracted using the mirVana miRNA isolation kit (Ambion, Austin, TX). Three micrograms of total RNA from the stomachs of 3 *H pylori*-infected mice were pooled, and the same was done for 3 control mice. miRNA microarray analysis with the pooled RNA samples from *H pylori*-infected mice and control mice was conducted by LC Sciences (www.lcsciences.com; Houston, TX). All data are Minimum Information About a Microarray Experiment (MIAME) compliant and have been deposited in the ArrayExpress database (accession number: E-MEXP-2239).

### Quantitative Reverse-Transcription Polymerase Chain Reaction of miRNAs

miRNA expression levels were analyzed by quantitative reverse-transcription polymerase chain reaction (RT-PCR) using the TaqMan microRNA assay for *miR-1*, *miR-133a*, and *miR-133b* (Applied Biosystems, Foster City, CA) in accordance with the manufacturer's instructions.

Expression levels were normalized against U6 RNA expression.

**Western Blotting**

Protein extracts were separated by sodium dodecyl sulfate/polyacrylamide gel electrophoresis and transferred onto nitrocellulose membranes. The membranes were hybridized with rabbit anti-human histone deacetylase 4 (HDAC4) polyclonal antibody (H-92: sc-11418; Santa Cruz Biotechnology, Santa Cruz, CA) and rabbit anti-human serum response factor (SRF) polyclonal antibody (G-20: sc-335; Santa Cruz Biotechnology).  $\beta$ -Actin was used as the internal control.

**Culture of C2C12 Mouse Myoblast Cells**

C2C12 mouse myoblast cells were obtained from the American Type Culture Collection (Manassas, VA), and cultured in Dulbecco's modified Eagle medium supplemented with 10% heat-inactivated fetal bovine serum (growth medium). Myogenic differentiation was induced by changing the growth medium to Dulbecco's modified Eagle medium containing 2% heat-inactivated horse serum (differentiation medium), as described previously.<sup>29</sup>

**Coculture With *H. pylori*, Transfection of anti-miRNA Inhibitors, and Treatment With Cytokines**

*H. pylori* bacteria (SS1) were added to C2C12 cells cultured with differentiation medium at a multiplicity of infection of 50 and cocultured for 12 hours, followed by isolation of total RNAs and proteins. Anti-miR-1 and anti-miR-133 inhibitors and a negative control were purchased from Ambion. Each anti-miRNA inhibitor is a chemically modified, single-stranded nucleic acid designed to bind to, and inhibit, a specific endogenous miRNA molecule. The inhibitors were transfected into C2C12 cells at a final concentration of 100 nmol/L using lipofectamine 2000 (Invitrogen, Carlsbad, CA) in accordance with the manufacturer's instructions. Forty-eight hours after transfection, the cells were collected and analyzed.

C2C12 cells were treated with the cytokines interleukin (IL)-1 $\beta$ , IL-13, and tumor necrosis factor (TNF)- $\alpha$  (R&D Systems, Inc, Minneapolis, MN) at concentrations of 10 pg/mL, 5 ng/mL, and 50 pg/mL, respectively, for 12 hours in accordance with the manufacturer's instructions.

**Immunostaining of C2C12 Cells With Ki-67**

C2C12 cells were fixed with 4% paraformaldehyde and permeabilized with 0.1% Triton X-100. They were then incubated with rat anti-mouse Ki-67 monoclonal antibody (Dako; diluted 1:50) overnight at 4°C, followed by Alexa Fluor 488 goat anti-mouse immunoglobulin G (Invitrogen), and examined using the fluorescence microscope. The cells were counterstained with DAPI.

**Cell Proliferation Enzyme-Linked Immunosorbent Assay Using Bromodeoxyuridine**

C2C12 cells were cultured in differentiation medium in a 96-well plate. They were cocultured with *H. pylori* (SS1) at a multiplicity of infection of 50, and labeled with bromodeoxyuridine (BrdU) for 12 hours. BrdU incorporation was quantified by colorimetric enzyme-linked immunosorbent assay (ELISA) in accordance with the manufacturer's instructions (Cell Proliferation ELISA, BrdU; Roche, Basel, Switzerland).

**Gastric Tissue Samples From Patients With *H. pylori* Infection**

Gastric tissue samples of the antral region of the stomach were obtained from patients with or without *H. pylori* infection by endoscopic biopsy at Keio University Hospital (Tokyo, Japan). *H. pylori* infection status was identified by the <sup>13</sup>C-urea breath test and/or serologic examination. Patients who had *H. pylori* eradication therapy were excluded. The average age of *H. pylori*-negative patients was 69.1 years (male/female, 6/2) and that of *H. pylori*-positive patients was 70.6 years (male/female, 11/

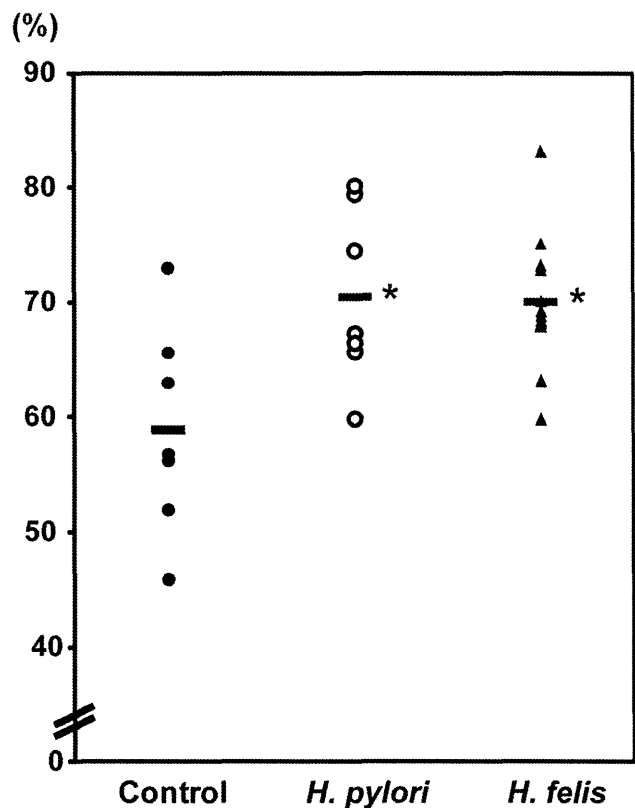


**Figure 1.** Gastric emptying in control mice and *Helicobacter*-infected mice. Gastric emptying rates (%) in control mice (n = 7) and mice chronically infected with *H. pylori* (n = 7) and *Helicobacter felis* (n = 13) were evaluated by measuring the amount of phenol red remaining in the stomach after oral administration. Gastric emptying was significantly increased in the stomachs of mice chronically infected with *H. pylori* and *H. felis* relative to control mice (\*P < .05).

3). This study was approved by Keio University School of Medicine Ethics Committee (No. 19-68-5) and entered in the University hospital Medical Information Network (UMIN) Clinical Trials Registry (UMIN 000001057). Informed consent was obtained from all patients before the examination.

### Statistical Analysis

Data were analyzed using the SPSS statistical software package version 17.0 (SPSS Inc, Chicago, IL). Differences at *P* values of less than .05 were considered significant.

## Results

### Significant Acceleration of Gastric Emptying in *Helicobacter*-Infected Mice

To evaluate gastric motility in *Helicobacter*-infected mice, we analyzed the gastric emptying rate of mice chronically infected with *H pylori* and *H felis* by measuring the amount of phenol red remaining in the stomach after oral administration. As shown in Figure 1, the gastric emptying rate was significantly increased in mice chronically infected with *H pylori* and *H felis* in comparison with control mice.

### Muscular Layer Hyperplasia in the Stomach of *H pylori*-Infected Mice

Histologic examination with H&E staining revealed active gastritis with infiltration of neutrophils and prominent thickening of the muscular layer in the gastric corpus of *H pylori*-infected mice (Figure 2A). The muscularis propria layer was significantly thicker in the stomachs of *H pylori*-infected mice than in those of control mice (Figure 2B).

To analyze proliferation of myocytes in the stomach, DAPI staining was performed, and the nuclei of myocytes were counted (Figure 3A). As shown in Figure 3B, the average number of myocytes in the muscular layer of the stomach was significantly increased in *H pylori*-infected mice in comparison with control mice, indicating the presence of myocyte hyperplasia in the former.

### Down-regulation of Muscle-Specific miRNAs in the Stomachs of *H pylori*-Infected Mice and *H pylori*-Positive Patients

To identify miRNAs that play important roles in *H pylori*-associated gastric disorders, we performed miRNA microarray analysis using gastric tissue samples

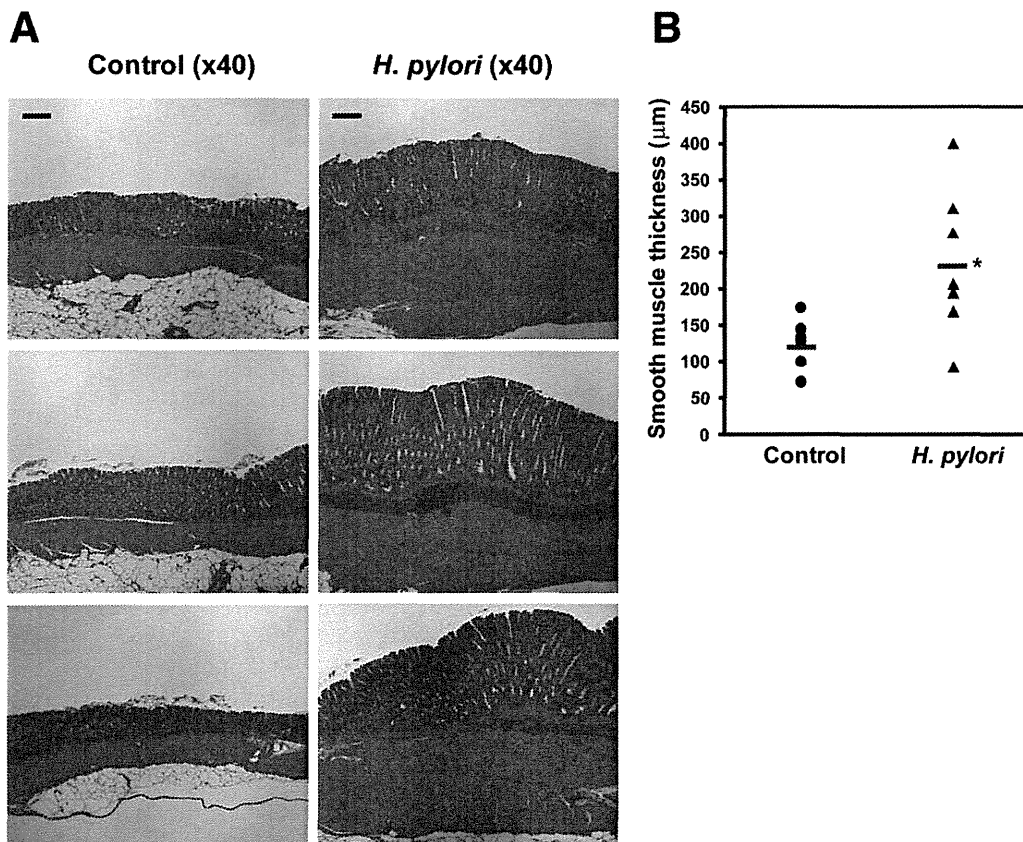


**Figure 2.** Histologic examination of the stomachs of control mice and mice chronically infected with *H pylori*. (A) Stomach tissues from uninfected control mice and mice infected with *H pylori* were stained with H&E and subjected to histologic examination (original magnification: 40 $\times$ ). The representative stomach tissues of 3 control mice and 3 infected mice are shown (scale bars, 100  $\mu$ m). (B) Comparison of gastric smooth muscle thickness between control mice (*n* = 7) and *H pylori*-infected mice (*n* = 7). The thickness of the muscularis propria layer was significantly increased in *H pylori*-infected mice relative to control mice (\**P* < .05).



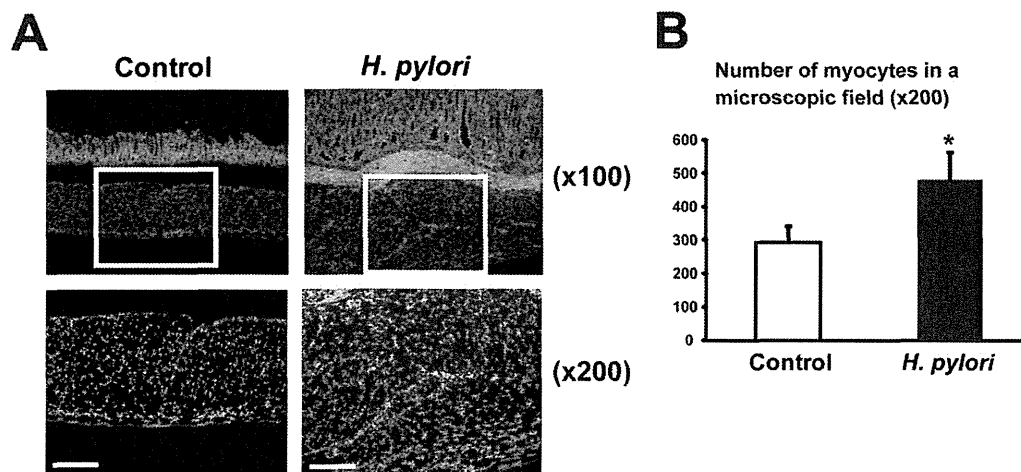


**Figure 3.** 4',6-Diamidino-2-phenylindole (DAPI) staining of the stomach of uninfected control mice and mice chronically infected with *H. pylori*. (A) Representative DAPI staining of control mice and infected mice. The muscular layer was randomly selected, as shown by the box (original magnification: 100 $\times$ ), in which the number of myocyte nuclei was counted at a magnification of 200 $\times$  (scale bars, 100  $\mu$ m). (B) The average number of myocytes in 2 randomly selected microscopic fields in the muscular layer of the stomach. The average number of myocytes in the muscular layer was significantly increased in *H. pylori*-infected mice ( $n = 7$ ) relative to control mice ( $n = 7$ ) (\* $P < .05$ ).

from *H. pylori*-infected mice and uninfected control mice. miRNA expression profiling revealed that 47 out of 470 miRNAs were differentially expressed in the gastric tissues of *H. pylori*-infected mice relative to control mice. Table 1 shows the 10 miRNAs with the greatest difference in expression. Interestingly, 3 of these 10 miRNAs—*miR-1*, *miR-133a*, and *miR-133b*—are known to be highly expressed in differentiated muscle tissues.<sup>27,28</sup> To confirm the microarray data, we performed quantitative RT-PCR for muscle-specific miRNAs. As shown in Figure 4A, the expression levels of *miR-1*, *miR-133a*, and *miR-133b* were markedly reduced in the stomachs of *H. pylori*-infected mice.

With respect to other miRNAs that were differentially expressed in the stomach of *H. pylori*-infected mice, *miR-206* is reported to be expressed in muscle tissues and down-regulated in estrogen receptor  $\alpha$ -positive human

breast cancer.<sup>34,35</sup> Recent studies have shown that *miR-217* and *miR-290* modulate cell senescence<sup>36,37</sup> and that *miR-122a* and *miR-146* function as novel tumor suppressors in cancer.<sup>38,39</sup>

We also examined the expression levels of muscle-specific miRNAs in clinical samples of the gastric antrum obtained by endoscopic biopsy from patients with or without *H. pylori* infection. These samples included muscularis mucosae and/or myoblast cells in the gastric epithelia. As shown in Figure 4B, the expression levels of *miR-1*, *miR-133a*, and *miR-133b* were significantly decreased in patients positive for *H. pylori* infection in comparison with those who were negative. These findings suggest that, in the muscularis mucosa and myoblast cells in gastric epithelia, as well as in the muscularis propria, muscle-specific miRNAs are down-regulated after *H. pylori* infection.

#### Increased Expression of HDAC4 and SRF in the Stomachs of *H. pylori*-Infected Mice

A recent study has shown that *miR-1* and *miR-133* specifically repress HDAC4 and SRF as their targets, respectively, thus contributing to the regulation of myoblast proliferation and differentiation.<sup>29,40</sup> Moreover, decreased expression of *miR-1* and *miR-133* has been observed in mouse and human cardiac hypertrophy.<sup>32</sup> These findings prompted us to investigate the expression levels of HDAC4 and SRF in the stomachs of *H. pylori*-infected mice. The results of Western blotting shown in Figure 5A demonstrate that the expression of HDAC4 and SRF was increased in the stomachs of *H. pylori*-infected mice relative to that in uninfected control mice, which is consistent with our finding that the expression levels of *miR-1* and *miR-133* were significantly reduced in the former.

**Table 1.** Summary of the Differentially Expressed miRNAs in the Stomach of *Helicobacter pylori*-Infected Mice

No.	miRNAs	Control	<i>H. pylori</i>	Fold change
1	<i>miR-206</i>	4013.2	17.5	0.004
2	<i>miR-217</i>	357.0	8.7	0.024
3	<i>miR-216b</i>	289.7	8.8	0.030
4	<i>miR-216a</i>	94.7	6.5	0.069
5	<i>miR-1</i>	18,214.4	4905.5	0.269
6	<i>miR-290</i>	100.4	365.1	3.635
7	<i>miR-122a</i>	83.5	269.8	3.230
8	<i>miR-133b</i>	3197.9	1228.2	0.384
9	<i>miR-133a</i>	2806.8	1080.3	0.385
10	<i>miR-146b</i>	397.3	955.7	2.406

NOTE. Data in control and *H. pylori* are average values of signal intensities of microarray analysis. Fold change represents the ratio of signal intensities of *H. pylori*/control. miRNA, microRNA.

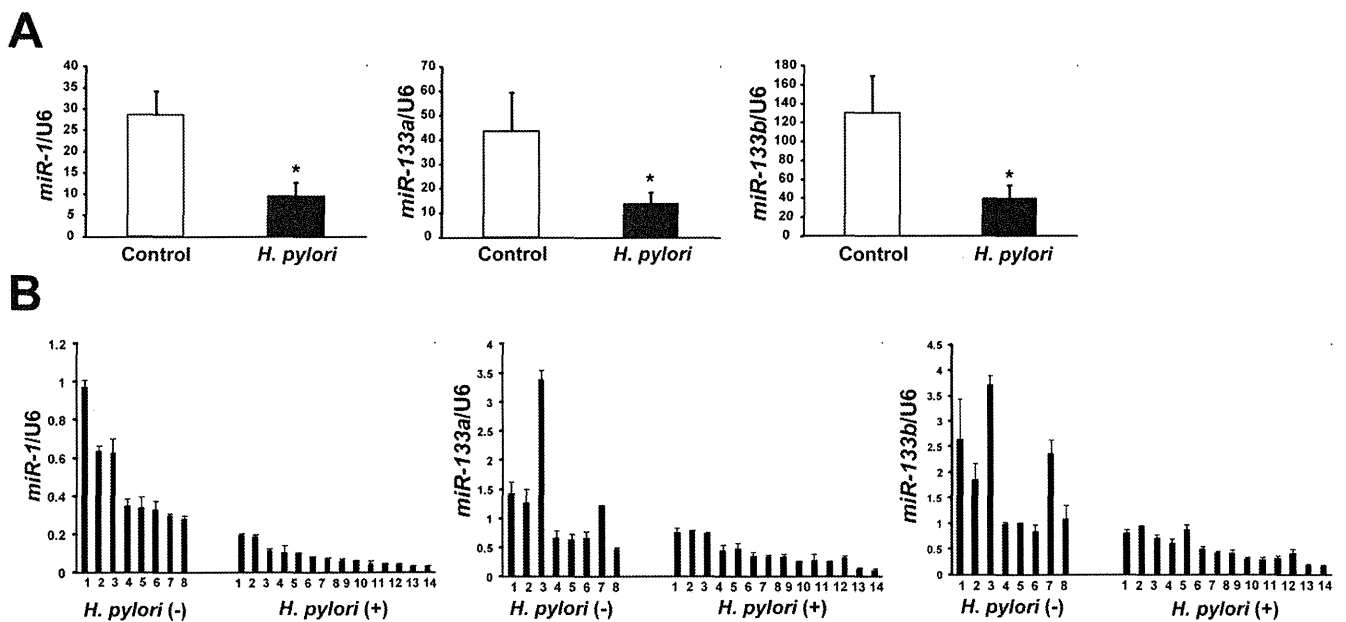


**Figure 4.** Expression levels of *miR-1* and *miR-133* in the stomachs of mice with *H. pylori* infection. (A) Expression levels of *miR-1*, *miR-133a*, and *miR-133b* were analyzed by quantitative RT-PCR using the TaqMan microRNA assay in the stomachs of control (open bar;  $n = 7$ ) and *H. pylori*-infected mice (solid bar;  $n = 7$ ). Expression levels were normalized against U6 RNA expression. All reactions were done in duplicate and expressed as mean  $\pm$  standard deviation. \* $P < .005$  compared with control. (B) Expression levels of *miR-1*, *miR-133a*, and *miR-133b* in clinical samples from the gastric antrum of patients with or without *H. pylori* infection. Expression levels of *miR-1*, *miR-133a*, and *miR-133b* were significantly decreased in patients positive for *H. pylori* infection ( $n = 14$ ), relative to patients who were negative ( $n = 8$ ) (*miR-1*,  $P < .005$ ; *miR-133a*,  $P < .05$ ; *miR-133b*,  $P < .01$ ).

To confirm these findings, we conducted in vitro validation with C2C12 mouse myoblast cells, which had been established by D. Yaffe and O. Saxel.<sup>41</sup> C2C12 is a mesenchymal cell line widely used as an in vitro model of muscle cell differentiation. The muscle-specific miRNAs, *miR-1* and *miR-133*, are induced during the differentiation of C2C12, thus allowing analysis of the expression patterns of muscle-specific miRNAs.<sup>28,29</sup> We transfected C2C12 cells with anti-*miR-1* and anti-*miR-133a* inhibitors and assessed the expression levels of the miRNAs and their targets by quantitative RT-PCR and Western blotting, respectively. As shown in Figure 5B, the expression levels of *miR-1* and *miR-133a* were significantly reduced in C2C12 cells after transfection with anti-*miR-1* and anti-*miR-133a*. After knockdown of *miR-1* and *miR-133a*, up-regulation of their targets, HDAC4 and SRF, was observed, indicating that inhibition of *miR-1* and *miR-133a* induced activation of HDAC4 and SRF (Figure 5B).

#### Significant Increase of C2C12 Myoblast Cell Proliferation After Coculture With *H. pylori*

The expression levels of muscle-specific miRNAs were analyzed in C2C12 myoblast cells after coculture with *H. pylori*. As shown in Figure 6A, the expression levels of *miR-1*, *miR-133a*, and *miR-133b* were significantly reduced in C2C12 cells cocultured with *H. pylori* relative to untreated C2C12 cells.

*H. pylori* infection induces an inflammatory response with increased levels of proinflammatory cytokines such

as IL-1 $\beta$  and TNF- $\alpha$ .<sup>42</sup> In addition, a recent study has shown that *miR-1* is down-regulated in IL-13-transgenic mice.<sup>43</sup> We investigated the expression levels of muscle-specific miRNAs after exogenous application of the cytokines IL-1 $\beta$ , IL-13, and TNF- $\alpha$ . Although *miR-1* expression was increased after application of TNF- $\alpha$ , and that of *miR-133a* was decreased after application of IL-13, the differences in miRNA expression induced by inflammatory cytokines were smaller than those induced by coculture with *H. pylori*. There was no significant difference in the expression level of *miR-133b* after application of cytokines. These results suggest that down-regulation of the muscle-specific miRNAs *miR-1*, *miR-133a*, and *miR-133b* is caused mainly by *H. pylori* itself, rather than inflammatory cytokines.

To further confirm the association between *H. pylori* infection and proliferation of myoblast cells, C2C12 myoblasts in active phases of the cell cycle were assessed by immunostaining with Ki-67. As shown in Figure 6B, Ki-67-positive C2C12 cells were sufficiently observed in cells cocultured with *H. pylori*, whereas there were a few positive cells in untreated cells. The number of Ki-67-positive cells was significantly increased upon coculture with *H. pylori* in comparison with cells cultured alone (Figure 6B).

We also performed ELISA with the BrdU assay to confirm the proliferation of C2C12 cells. As shown in Figure 6B, the rate of BrdU incorporation was signifi-

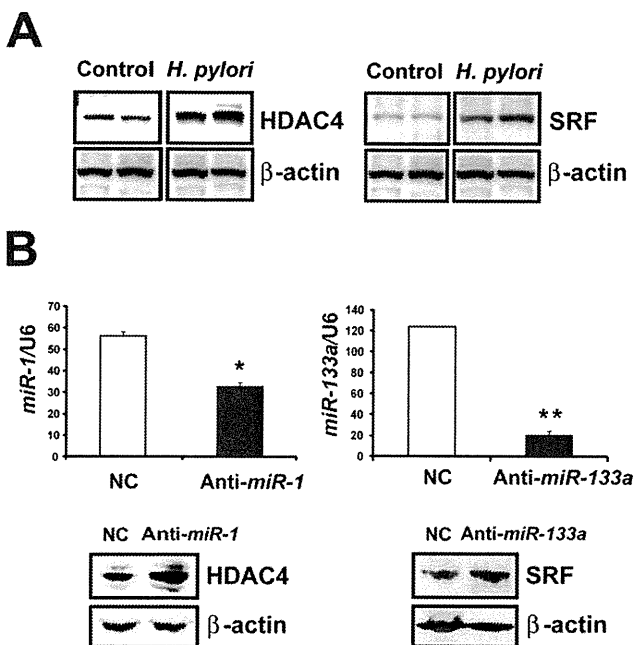


**Figure 5.** Expression levels of HDAC4 and SRF in the stomachs of control and *H. pylori*-infected mice and C2C12 mouse myoblast cells. (A) Expression levels of HDAC4 and SRF in the stomachs of control and *H. pylori*-infected mice were analyzed by Western blotting.  $\beta$ -Actin was used as the internal control. (B) C2C12 mouse myoblast cells were transfected with a negative control (NC; open bar) and inhibitors of *miR-1* and *miR-133a* (solid bar), and the expression levels of *miR-1* and *miR-133a* were confirmed by quantitative RT-PCR. Expression levels of HDAC4 and SRF were assessed by Western blotting. U6 RNA and  $\beta$ -actin were used as the internal controls. The quantitative RT-PCR reactions were done in triplicate and expressed as mean  $\pm$  standard deviation. \* $P < .05$ , \*\* $P < .01$  compared with NC.

cantly increased in C2C12 cells cocultured with *H. pylori* relative to cells that were cultured alone, indicating that coculture with *H. pylori* induces proliferation of C2C12 myoblasts.

## Discussion

Little is known about the molecular mechanism underlying the pathogenesis of functional GI disorders, including FD. Our present results demonstrate that gastric emptying was accelerated in mice infected with *Helicobacter*. Moreover, the miRNA expression profile revealed that the muscle-specific miRNAs, *miR-1* and *miR-133*, were significantly down-regulated in the stomachs of *H. pylori*-infected mice. We were able to show, for the first time, that chronic infection with *H. pylori* induces down-regulation of muscle-specific miRNAs and hyperplasia of muscle cells in the stomach, which may lead to dysfunction of gastric emptying.

Although recently it has been reported that patients with FD frequently have delayed gastric emptying,<sup>9-11</sup> our study using a mouse model showed that gastric emptying was accelerated after chronic infection with *H. pylori*. It should be borne in mind that the gastric emp-

tying rate examined in the present study was liquid emptying, which is physiologically different from emptying of a solid meal. Therefore, the clinical implications of our results may not necessarily reflect the clinically more relevant gastric emptying of nutrient solids. Rapid gastric emptying of a liquid meal has been reported in patients with type 2 diabetes, even though that of nutrient solids may be normal or delayed.<sup>44-46</sup> Recent clinical studies indicate that a subset of FD patients may have impaired gastric accommodation, which may be associated with liquid gastric emptying.<sup>47,48</sup> These findings suggest that enhanced liquid emptying may be due to impaired gastric accommodation rather than increased muscular propulsive contraction. Impaired gastric accommodation may contribute to symptom generation such as early satiety observed in postprandial distress syndrome. Studies of the gastric emptying of solids will be necessary to further investigate the gastric motility disorders associated with *H. pylori* infection.

We showed that reduced expression of muscle-specific miRNAs led to activation of their targets, HDAC4 and SRF, in the stomachs of *H. pylori*-infected mice and also in C2C12 mouse myoblast cells. HDAC4, a transcriptional repressor of muscle gene expression, has been shown to inhibit muscle differentiation.<sup>49,50</sup> SRF is a transcription factor that binds to the serum response element, a sequence that mediates the transient response of many cellular genes to growth stimulation. Increased expression of HDAC4 and SRF is thought to impair the differentiation and proliferation of muscle cells, possibly causing hyperplasia of smooth muscle cells and disorders of gastric motility.

The *in vitro* study using C2C12 myoblast cells also demonstrated that coculture with *H. pylori* induced down-regulation of *miR-1* and *miR-133* and increased cell proliferation. Our data indicate that down-regulation of muscle-specific miRNAs is probably caused by *H. pylori* itself rather than inflammatory cytokines. These findings raise the possibility that *H. pylori* alone may elaborate mediators capable of enhancing the proliferation of muscle cells. Further studies will be necessary to clarify the systems responsible for regulation of miRNA expression and the proliferation and differentiation of muscle cells in the stomach through the direct and indirect effects of chronic *H. pylori* infection.

We obtained samples of gastric tissue from mice in which *miR-1* had been knocked out by targeted deletion and examined them histologically by H&E staining.<sup>30</sup> Although this model is characterized by a striking myocyte cell-cycle abnormality that leads to hyperplasia of the heart, we observed no significant difference in thickness of muscular layer in the stomach between control mice and mice lacking *miR-1* (data not shown). This suggests that hyperplasia of myocytes in the stomach might require down-regulation of other muscle-specific

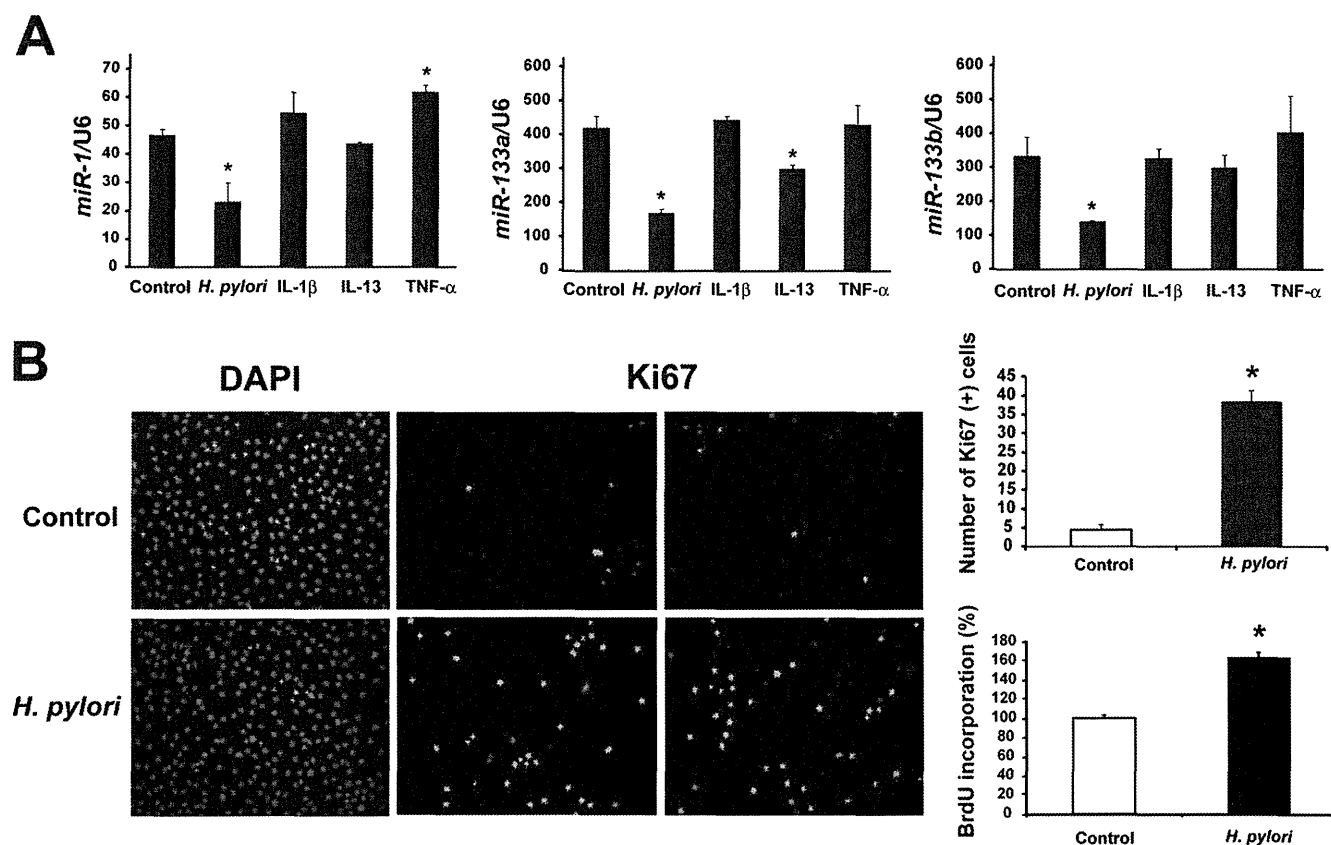


**Figure 6.** Expression levels of muscle-specific miRNAs and proliferation of C2C12 cells after coculture with *H. pylori*. (A) Expression levels of *miR-1*, *miR-133a*, and *miR-133b* were analyzed by quantitative RT-PCR in C2C12 cells after coculture with *H. pylori* and treatment with IL-1 $\beta$ , IL-13, and TNF- $\alpha$ . Expression levels were normalized against that of U6 RNA. All reactions were done in duplicate and expressed as mean  $\pm$  standard deviation. \* $P < .05$  compared with control. (B) Cell proliferation assay was performed by immunostaining of C2C12 cells for Ki-67 (original magnification: 200 $\times$ ). The cells were counterstained with DAPI. The numbers of Ki-67-positive cells among control cells and cells cocultured with *H. pylori* were counted. BrdU assay was performed in C2C12 cells cocultured with *H. pylori* at a multiplicity of infection of 50. BrdU incorporation was quantified by colorimetric ELISA assay. \* $P < .001$  compared with control.

miRNAs such as *miR-133a* and *miR-133b*, in addition to disruption of *miR-1*.

A recent study has shown that expression of *miR-29a* was increased in the small bowel and colon tissues of patients with IBS. Increased expression of *miR-29a* suppresses the *glutamine synthetase (GLUL)* gene as its target and regulates intestinal membrane permeability in patients with IBS.<sup>26</sup> Moreover, Kapeller et al<sup>25</sup> have indicated an association of functional variants in the *miR-510* binding site of the *serotonin receptor type 3E (HTR3E)* gene with diarrhea-predominant IBS. These findings, taken together with our present results, suggest that miRNAs may play important roles in the pathogenesis of functional GI disorders and could be novel therapeutic targets in patients with FD and IBS.

In conclusion, chronic infection with *H. pylori* has been shown to induce down-regulation of muscle-specific miRNAs with activation of their targets HDAC4 and SRF, which may lead to muscular layer hyperplasia and dysfunction of gastric emptying. Further human studies will be necessary to validate the association between ab-

errant expression of muscle-specific miRNAs and the gastric motility disorder associated with *H. pylori* infection.

## References

- Houghton J, Wang TC. *Helicobacter pylori* and gastric cancer: a new paradigm for inflammation-associated epithelial cancers. *Gastroenterology* 2005;128:1567-1578.
- Suzuki H, Hibi T, Marshall BJ. *Helicobacter pylori*: present status and future prospects in Japan. *J Gastroenterol* 2007;42:1-15.
- Cover TL, Blaser MJ. *Helicobacter pylori* in health and disease. *Gastroenterology* 2009;136:1863-1873.
- Hatakeyama M. Linking epithelial polarity and carcinogenesis by multitasking *Helicobacter pylori* virulence factor CagA. *Oncogene* 2008;27:7047-7054.
- Hatakeyama M. *Helicobacter pylori* and gastric carcinogenesis. *J Gastroenterol* 2009;44:239-248.
- Tucci A, Corinaldesi R, Stanghellini V, et al. *Helicobacter pylori* infection and gastric function in patients with chronic idiopathic dyspepsia. *Gastroenterology* 1992;103:768-774.
- Saslow SB, Thumshirn M, Camilleri M, et al. Influence of *H. pylori* infection on gastric motor and sensory function in asymptomatic volunteers. *Dig Dis Sci* 1998;43:258-264.

8. Mearin F, de Ribot X, Balboa A, et al. Does *Helicobacter pylori* infection increase gastric sensitivity in functional dyspepsia? *Gut* 1995;37:47–51.
9. Stanghellini V, Tosetti C, Paternico A, et al. Risk indicators of delayed gastric emptying of solids in patients with functional dyspepsia. *Gastroenterology* 1996;110:1036–1042.
10. Maes BD, Ghooos YF, Hiele MI, et al. Gastric emptying rate of solids in patients with nonulcer dyspepsia. *Dig Dis Sci* 1997;42:1158–1162.
11. Sarnelli G, Caenepeel P, Geypens B, et al. Symptoms associated with impaired gastric emptying of solids and liquids in functional dyspepsia. *Am J Gastroenterol* 2003;98:783–788.
12. Talley NJ, Verlinden M, Jones M. Can symptoms discriminate among those with delayed or normal gastric emptying in dysmotility-like dyspepsia? *Am J Gastroenterol* 2001;96:1422–1428.
13. Bredenoord AJ, Chial HJ, Camilleri M, et al. Gastric accommodation and emptying in evaluation of patients with upper gastrointestinal symptoms. *Clin Gastroenterol Hepatol* 2003;1:264–272.
14. Delgado-Aros S, Camilleri M, Cremonini F, et al. Contributions of gastric volumes and gastric emptying to meal size and postmeal symptoms in functional dyspepsia. *Gastroenterology* 2004;127:1685–1694.
15. Sykora J, Malan A, Zahlava J, et al. Gastric emptying of solids in children with *H pylori*-positive and *H pylori*-negative non-ulcer dyspepsia. *J Pediatr Gastroenterol Nutr* 2004;39:246–252.
16. Lee KJ, Demarchi B, Demedts I, et al. A pilot study on duodenal acid exposure and its relationship to symptoms in functional dyspepsia with prominent nausea. *Am J Gastroenterol* 2004;99:1765–1773.
17. He L, Hannon GJ. MicroRNAs: small RNAs with a big role in gene regulation. *Nat Rev Genet* 2004;5:522–531.
18. Saito Y, Liang G, Egger G, et al. Specific activation of microRNA-127 with down-regulation of the proto-oncogene BCL6 by chromatin-modifying drugs in human cancer cells. *Cancer Cell* 2006;9:435–443.
19. Calin GA, Croce CM. MicroRNA signatures in human cancers. *Nat Rev Cancer* 2006;6:857–866.
20. Calin GA, Croce CM. Chromosomal rearrangements and microRNAs: a new cancer link with clinical implications. *J Clin Invest* 2007;117:2059–2066.
21. Saito Y, Suzuki H, Hibi T. The role of microRNAs in gastrointestinal cancers. *J Gastroenterol* 2009;44(Suppl 19):18–22.
22. Saito Y, Jones PA. Epigenetic activation of tumor suppressor microRNAs in human cancer cells. *Cell Cycle* 2006;5:2220–2222.
23. Saito Y, Friedman JM, Chihara Y, et al. Epigenetic therapy up-regulates the tumor suppressor microRNA-126 and its host gene EGFL7 in human cancer cells. *Biochem Biophys Res Commun* 2009;379:726–731.
24. Saito Y, Suzuki H, Tsugawa H, et al. Chromatin remodeling at Alu repeats by epigenetic treatment activates silenced microRNA-512-5p with down-regulation of Mcl-1 in human gastric cancer cells. *Oncogene* 2009;28:2738–2744.
25. Kapeller J, Houghton LA, Monnikes H, et al. First evidence for an association of a functional variant in the microRNA-510 target site of the serotonin receptor-type 3E gene with diarrhea predominant irritable bowel syndrome. *Hum Mol Genet* 2008;17:2967–2977.
26. Zhou Q, Souba WW, Croce CM, et al. MicroRNA-29a regulates intestinal membrane permeability in patients with irritable bowel syndrome. *Gut* 2009;59:775–784.
27. Sempere LF, Freemantle S, Pitha-Rowe I, et al. Expression profiling of mammalian microRNAs uncovers a subset of brain-expressed microRNAs with possible roles in murine and human neuronal differentiation. *Genome Biol* 2004;5:R13.
28. Rao PK, Kumar RM, Farkhondeh M, et al. Myogenic factors that regulate expression of muscle-specific microRNAs. *Proc Natl Acad Sci U S A* 2006;103:8721–8726.
29. Chen JF, Mandel EM, Thomson JM, et al. The role of microRNA-1 and microRNA-133 in skeletal muscle proliferation and differentiation. *Nat Genet* 2006;38:228–233.
30. Zhao Y, Ransom JF, Li A, et al. Dysregulation of cardiogenesis, cardiac conduction, and cell cycle in mice lacking miRNA-1-2. *Cell* 2007;129:303–317.
31. Sayed D, Hong C, Chen IY, et al. MicroRNAs play an essential role in the development of cardiac hypertrophy. *Circ Res* 2007;100:416–424.
32. Care A, Catalucci D, Felicetti F, et al. MicroRNA-133 controls cardiac hypertrophy. *Nat Med* 2007;13:613–618.
33. Suzuki S, Suzuki H, Horiguchi K, et al. Delayed gastric emptying and disruption of the interstitial cells of Cajal network after gastric ischaemia and reperfusion. *Neurogastroenterol Motil* 2009;22:585–593.
34. Kim HK, Lee YS, Sivaprasad U, et al. Muscle-specific microRNA miR-206 promotes muscle differentiation. *J Cell Biol* 2006;174:677–687.
35. Kondo N, Toyama T, Sugiyama H, et al. miR-206 expression is down-regulated in estrogen receptor  $\alpha$ -positive human breast cancer. *Cancer Res* 2008;68:5004–5008.
36. Menghini R, Casagrande V, Cardellini M, et al. MicroRNA 217 modulates endothelial cell senescence via silent information regulator 1. *Circulation* 2009;120:1524–1532.
37. Pitto L, Rizzo M, Simili M, et al. miR-290 acts as a physiological effector of senescence in mouse embryo fibroblasts. *Physiol Genomics* 2009;39:210–218.
38. Wang X, Lam EK, Zhang J, et al. MicroRNA-122a functions as a novel tumor suppressor downstream of adenomatous polyposis coli in gastrointestinal cancers. *Biochem Biophys Res Commun* 2009;387:376–380.
39. Hurst DR, Edmonds MD, Scott GK, et al. Breast cancer metastasis suppressor 1 up-regulates miR-146, which suppresses breast cancer metastasis. *Cancer Res* 2009;69:1279–1283.
40. Liu N, Bezprozvannaya S, Williams AH, et al. microRNA-133a regulates cardiomyocyte proliferation and suppresses smooth muscle gene expression in the heart. *Genes Dev* 2008;22:3242–3254.
41. Yaffe D, Saxel O. Serial passaging and differentiation of myogenic cells isolated from dystrophic mouse muscle. *Nature* 1977;270:725–727.
42. Mejias-Luque R, Linden SK, Garrido M, et al. Inflammation modulates the expression of the intestinal mucins MUC2 and MUC4 in gastric tumors. *Oncogene* 2010;29:1753–1762.
43. Lu TX, Munitz A, Rothenberg ME. MicroRNA-21 is up-regulated in allergic airway inflammation and regulates IL-12p35 expression. *J Immunol* 2009;182:4994–5002.
44. Phillips WT, Schwartz JG, McMahan CA. Rapid gastric emptying in patients with early non-insulin-dependent diabetes mellitus. *N Engl J Med* 1991;324:130–131.
45. Phillips WT, Schwartz JG, McMahan CA. Rapid gastric emptying of an oral glucose solution in type 2 diabetic patients. *J Nucl Med* 1992;33:1496–1500.
46. Weytjens C, Keymeulen B, Van Haleweyn C, et al. Rapid gastric emptying of a liquid meal in long-term type 2 diabetes mellitus. *Diabet Med* 1998;15:1022–1027.
47. Tack J, Demedts I, Dehondt G, et al. Clinical and pathophysiological characteristics of acute-onset functional dyspepsia. *Gastroenterology* 2002;122:1738–1747.
48. Kindt S, Tack J. Impaired gastric accommodation and its role in dyspepsia. *Gut* 2006;55:1685–1691.
49. Lu J, McKinsey TA, Zhang CL, et al. Regulation of skeletal myogenesis by association of the MEF2 transcription factor with class II histone deacetylases. *Mol Cell* 2000;6:233–244.